Semiconductor Devices

THIRD EDITION

S. M. Sze and M. K. Lee

Chapter 9

Light-Emitting Diodes and Lasers

應用在λ:0.3~1.5um, 可見光 ~ IR

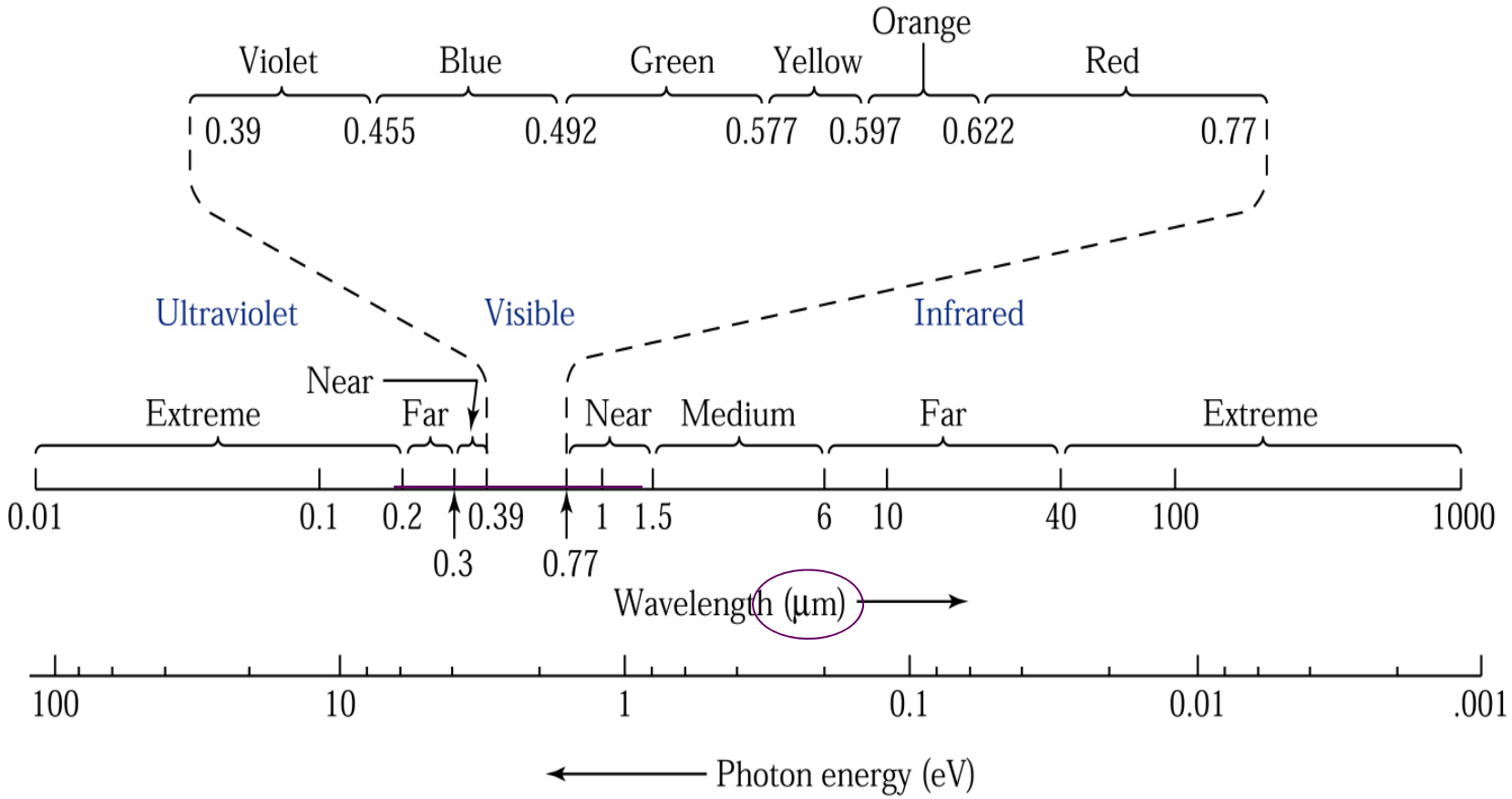

Figure 9.1. Chart of the electromagnetic spectrum from the ultraviolet region to the infrared region.

Figure 9.2.
The three basic transition processes between two energy levels.[1] Black dots indicated the state of the atom. The initial state is at the left; the final state, after the transition, is at the right. (*a*) Absorption. (*b*) Spontaneous emission. (*c*) **Stimulated emission**.

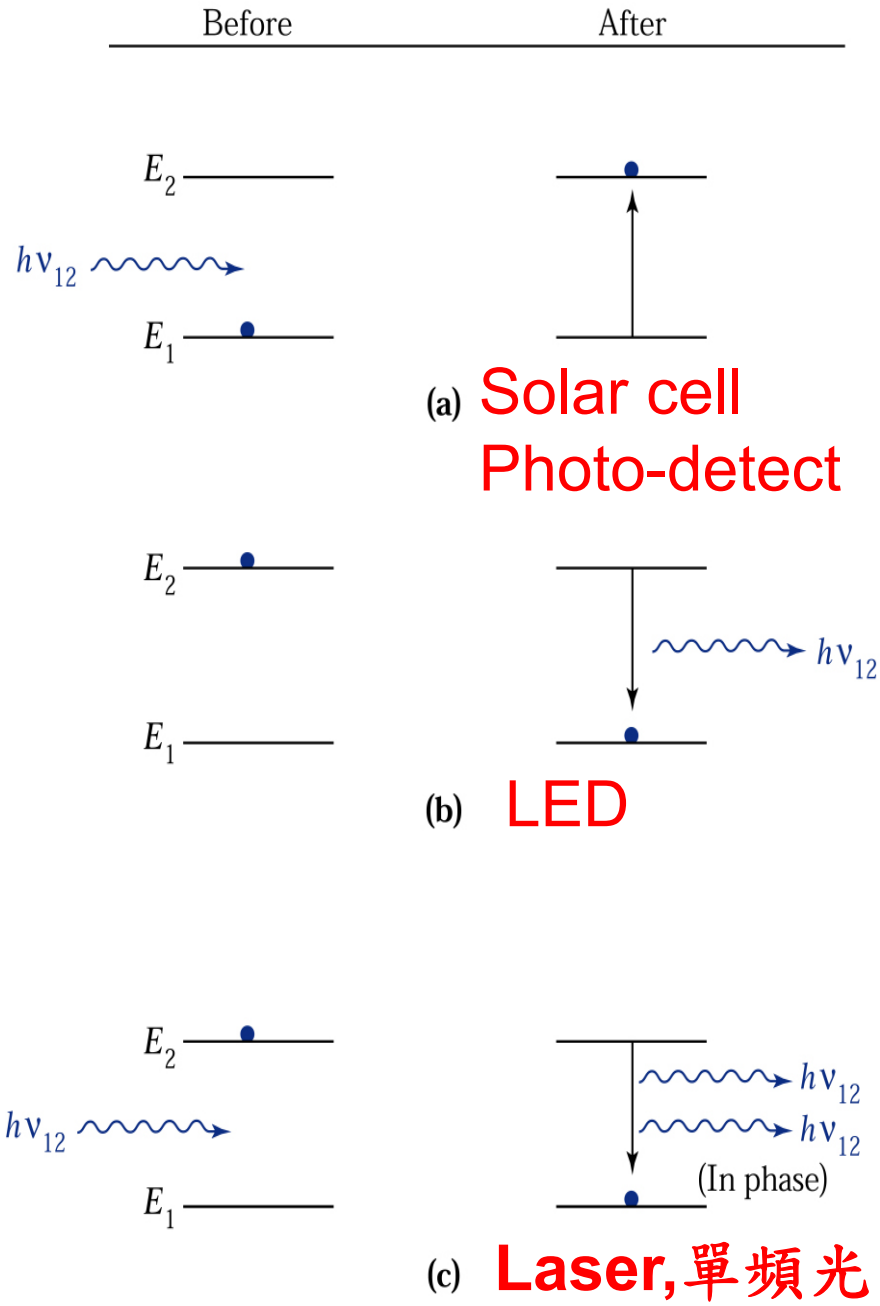

光子與電子之相互作用

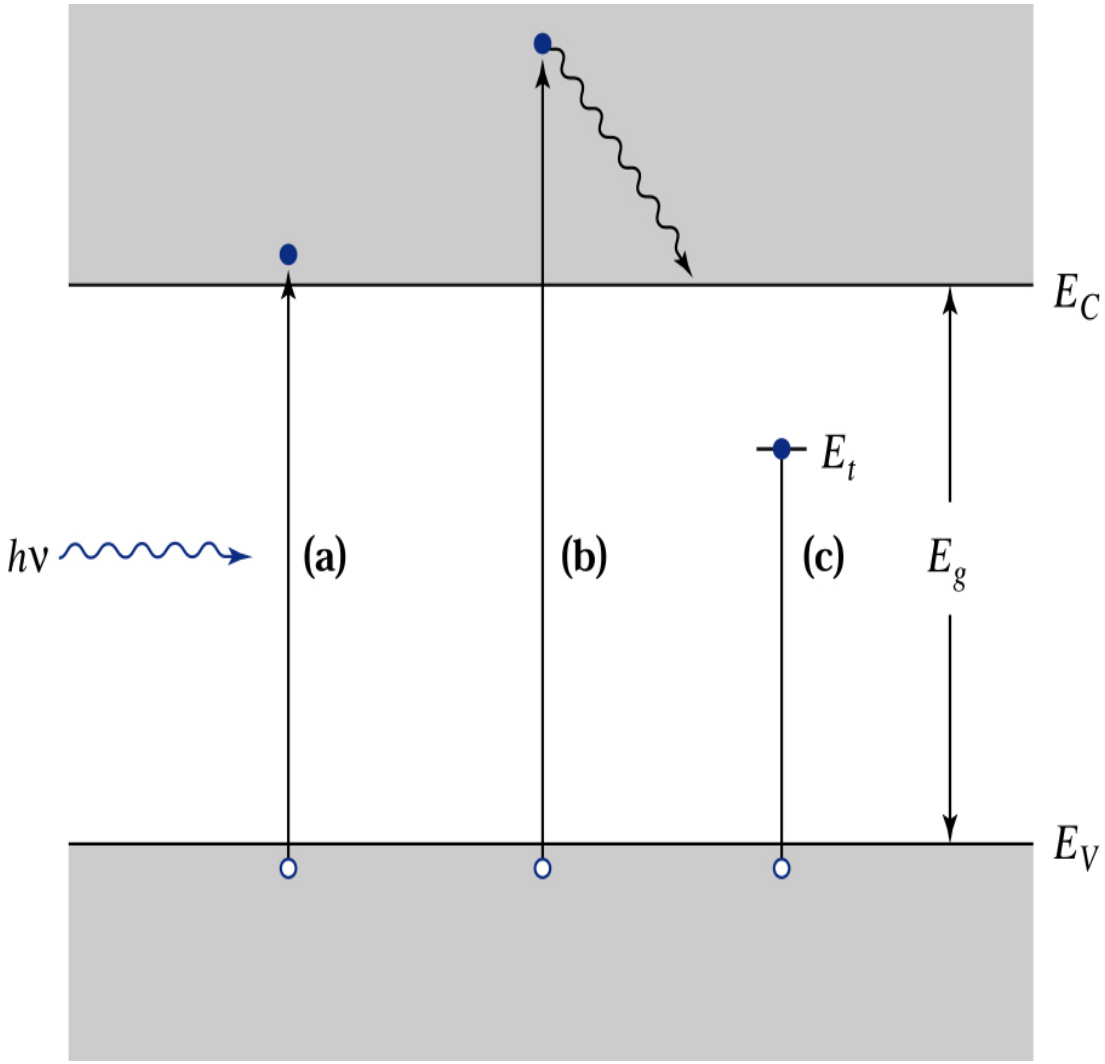

Figure 9.3. Optical absorption for (*a*) $h_v = E_g$, (*b*) $h_v > E_g$, and (*c*) $h_v < E_g$.

intrinsic **extrinsic**

Figure 9.4.
Optical absorption.
(*a*) Semiconductor under illumination. (*b*) Exponential decay of photon flux.

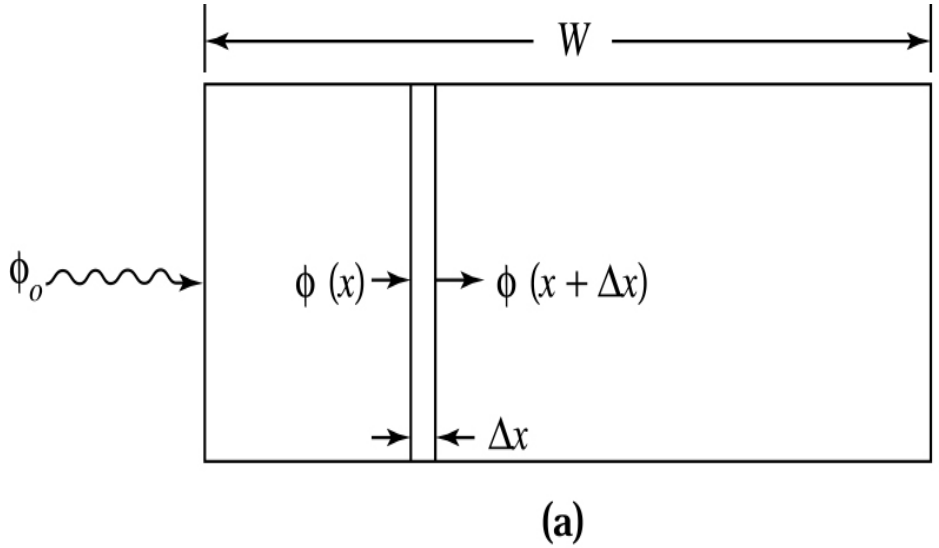

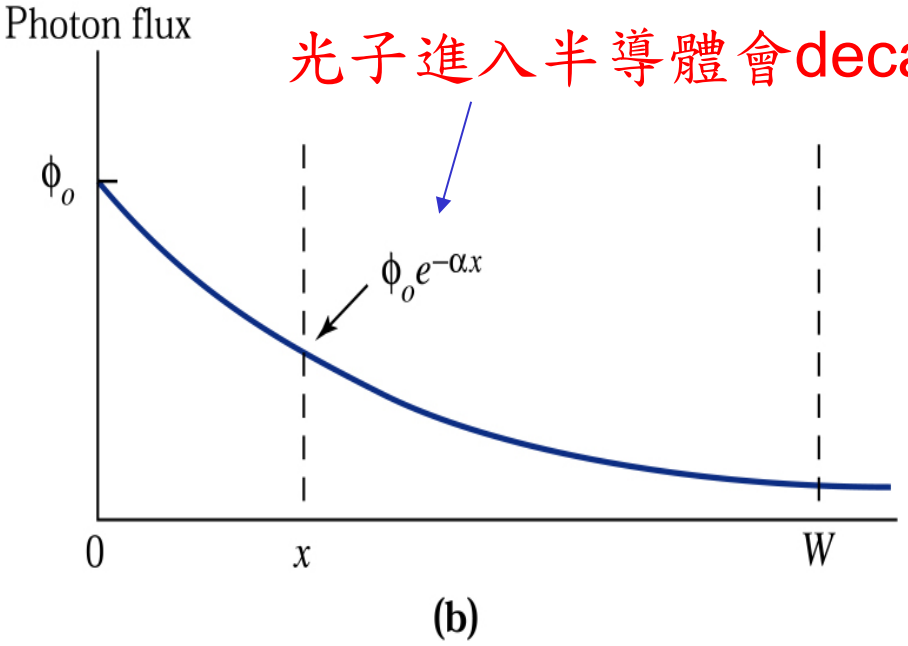

α:吸收係數

Figure 9.5.
Optical absorption coefficients for various semiconductor materials.[2]. The value in the parenthesis is the cutoff wavelength.

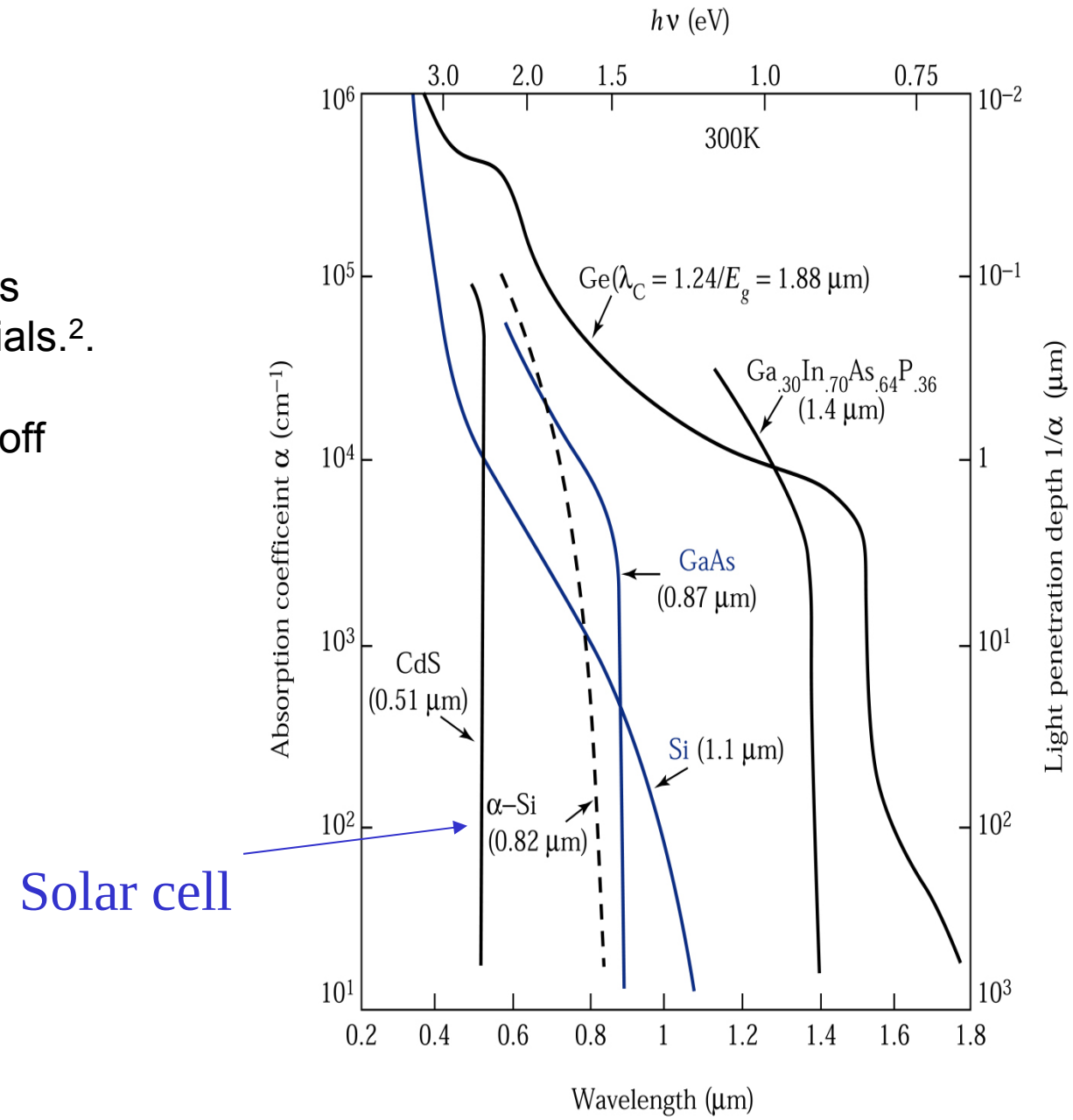

(a) forward
(b) recombination
(c) Double heterojunction

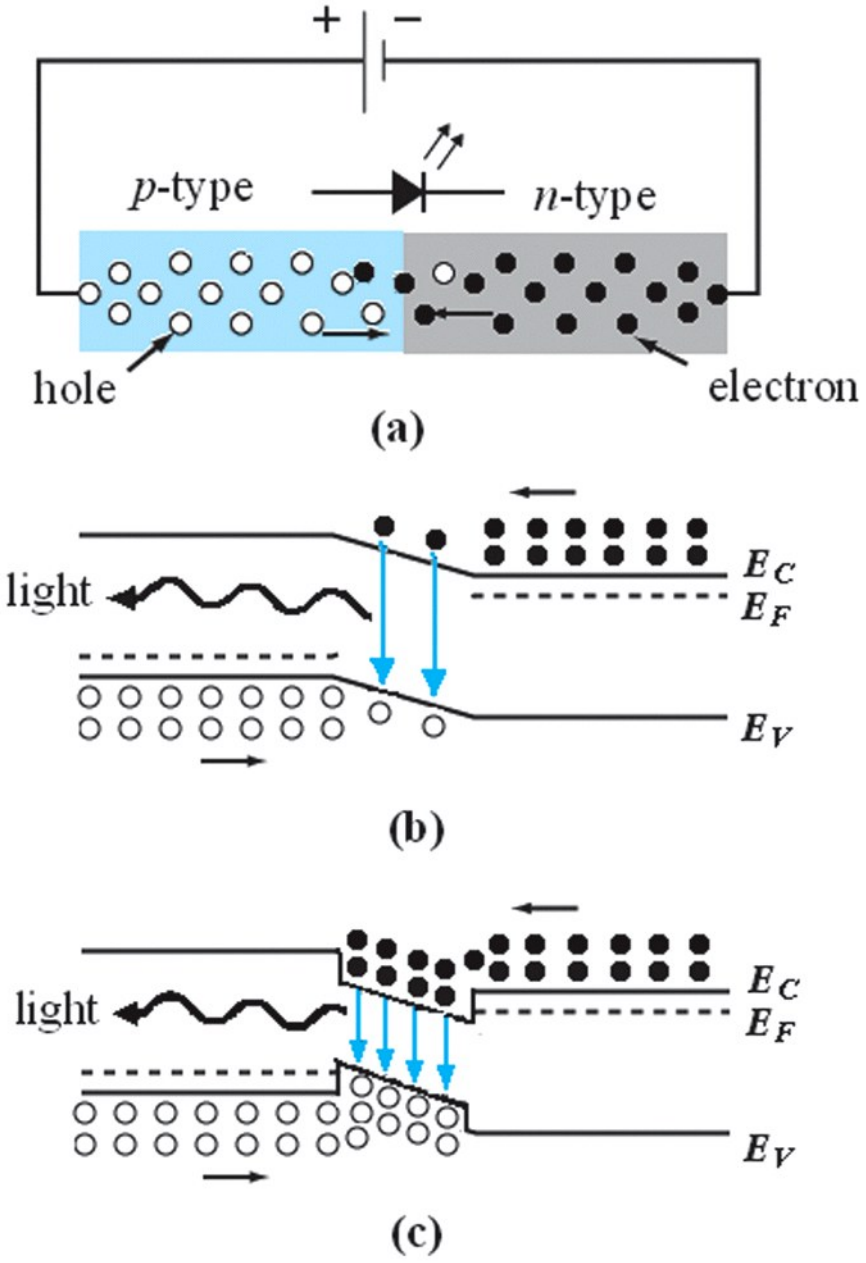

Figure 9.6

Figure 9.7.
Basic structure of a flat-diode LED and the effects of (*a*) an opaque substrate ($GaAs_{1-y}P_y$) and (*b*) a transparent substrate (GaP) on photons emitted at the *p-n* junction.[5]

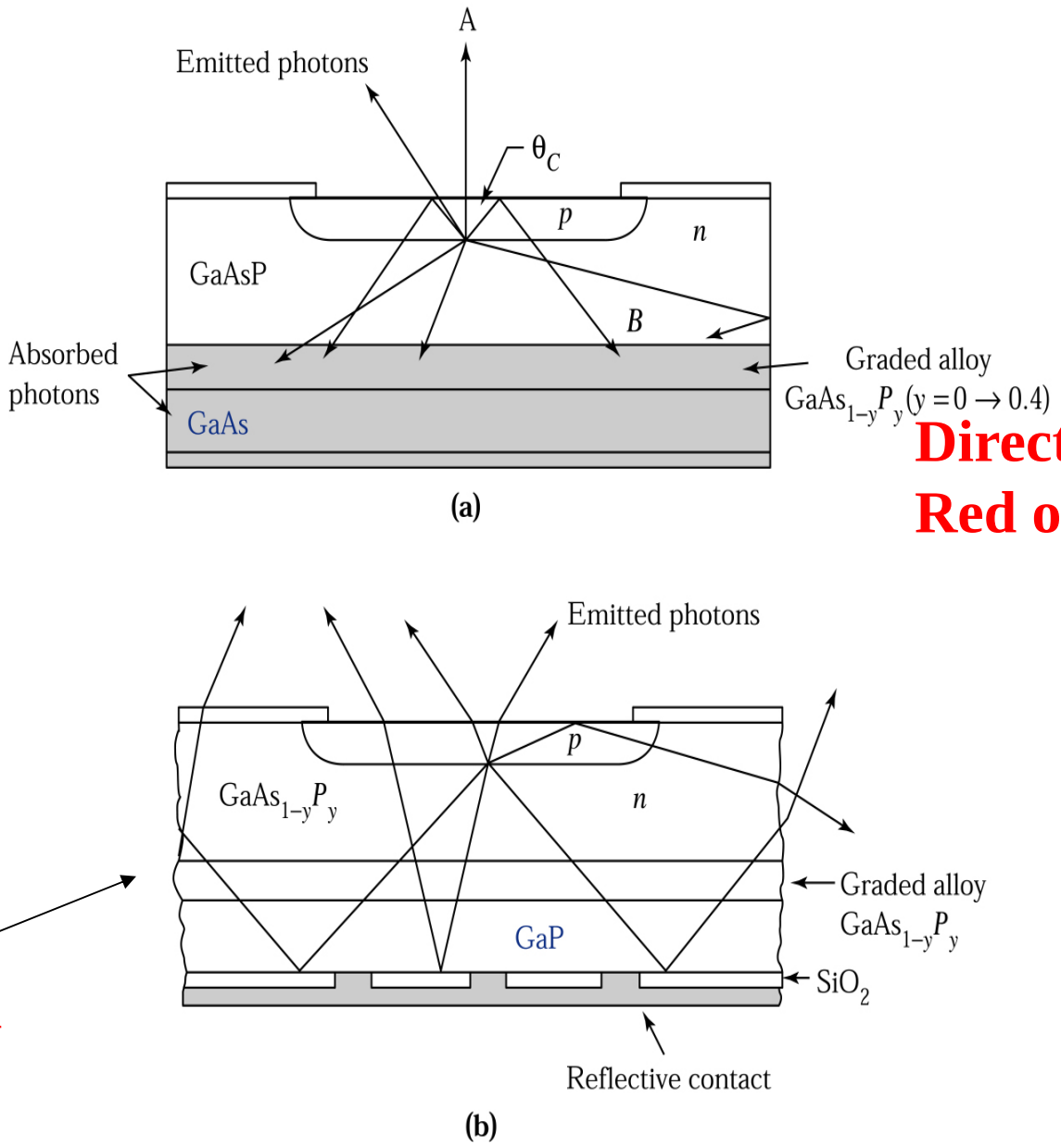

Direct, Red only

Indirect, Orange, yellow, green

Figure 9.8. Semiconductors of interest as **visible LEDs**. Figure includes relative response of the human eye.

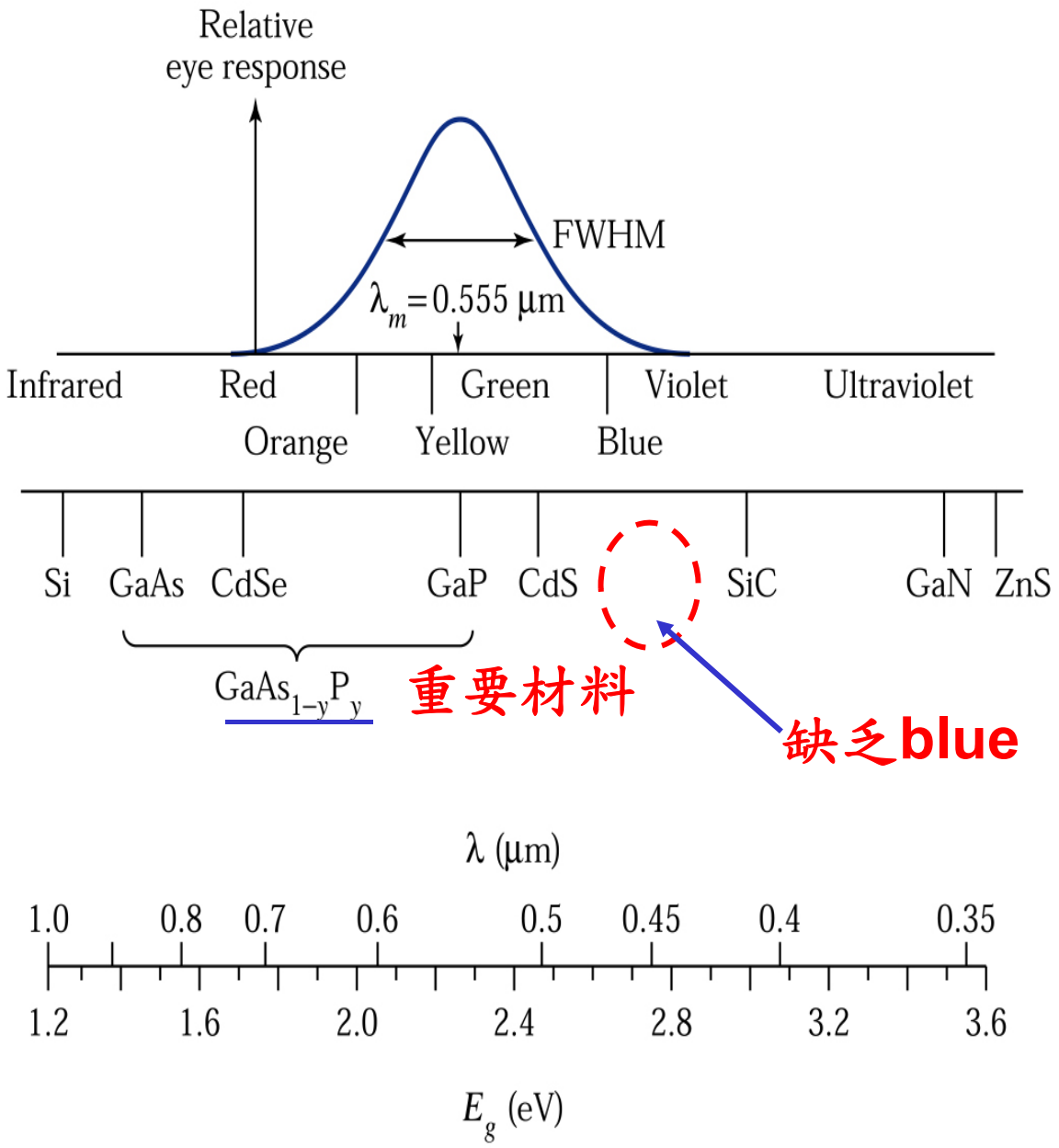

TABLE 1 COMMON III-V MATERIALS USED TO PRODUCE LEDS AND THEIR EMISSION WAVELENGTHS

Material	Wavelength (nm)
InAsSbP/InAs	4200
InAs	3800
GaInAsP/GaSb	2000
GaSb	1800
$Ga_xIn_{1-x}As_{1-y}P_y$	1100-1600
$Ga_{0.47}In_{0.53}As$	1550
$Ga_{0.27}In_{0.73}As_{0.63}P_{0.37}$	1300
GaAs:Er,InP:Er	1540
Si:C	1300
GaAs:Yb,InP:Yb	1000
$Al_xGa_{1-x}As$:Si	650-940
GaAs:Si	940
$Al_{0.11}Ga_{0.89}As$:Si	830
$Al_{0.4}Ga_{0.6}As$:Si	650
$GaAs_{0.6}P_{0.4}$	660
$GaAs_{0.4}P_{0.6}$	620
$GaAs_{0.15}P_{0.85}$	590
$(Al_xGa_{1-x})_{0.5}In_{0.5}P$	655
GaP	690
GaP:N	550-570
$Ga_xIn_{1-x}N$	340,430,590
SiC	400-460
BN	260,310,490

Table 9.1

Figure 9.9.
(*a*) Compositional dependence for the direct- and indirect-energy bandgap for $GaAs_{1-y}P_y$. (*b*) The alloy compositions shown correspond to **red (y = 0.4), orange (0.65), yellow (0.85), and green light (1,0).**[3]

Y>0.45時須藉G-R Center 產生光(如N)

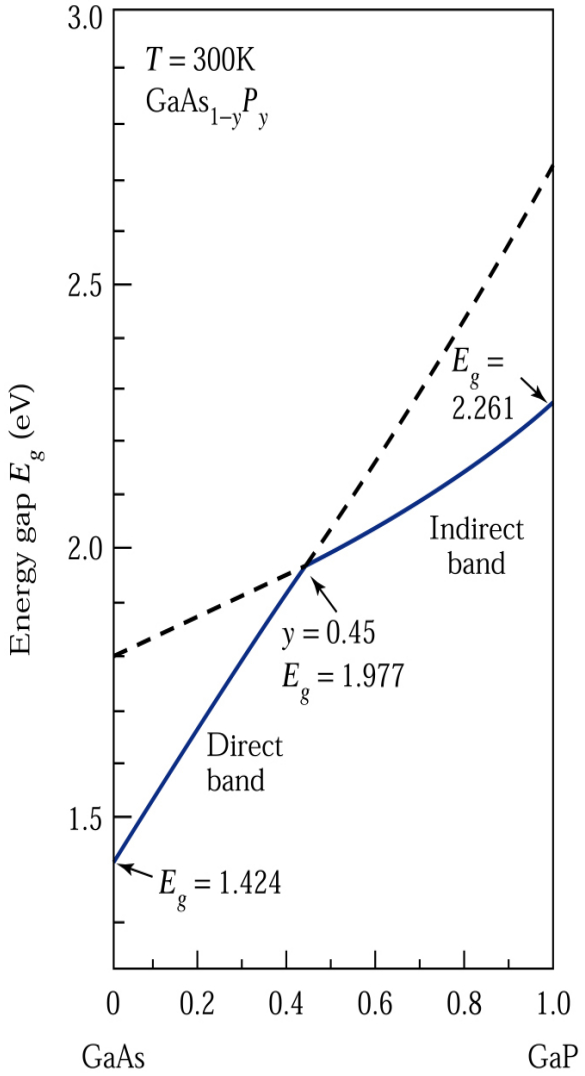

(a)

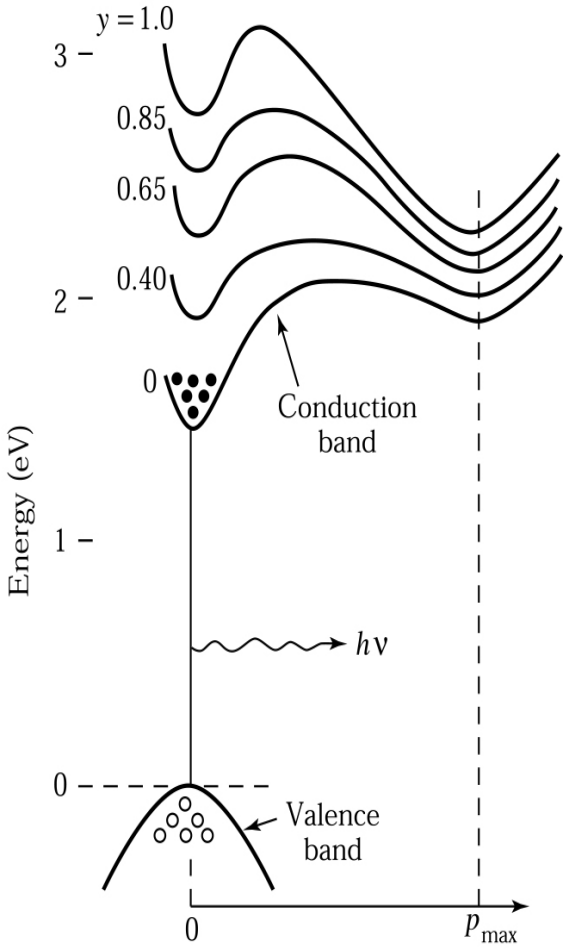

(b)

Radiative recombination
In indirect bandgap

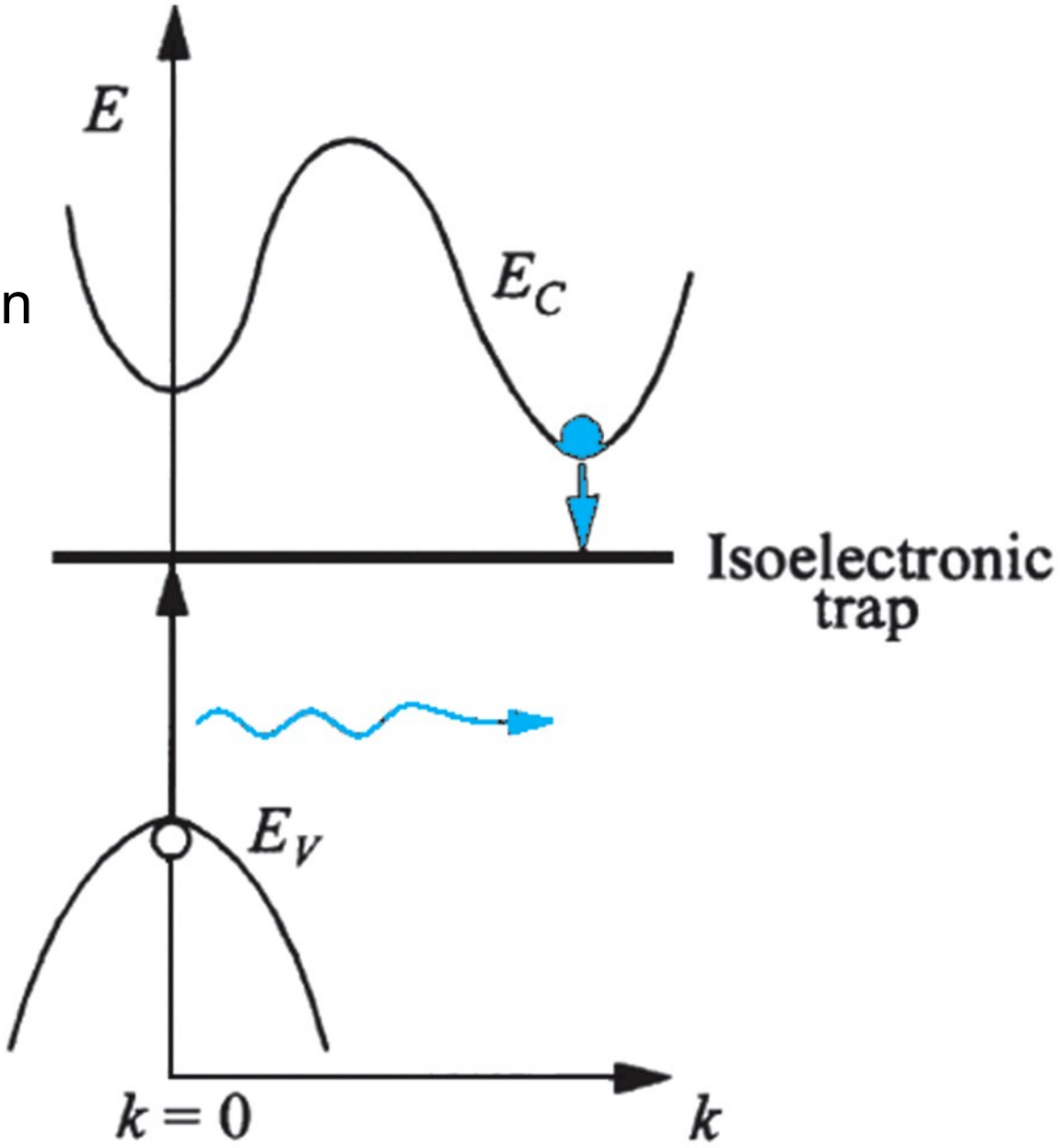

Figure 9.10a

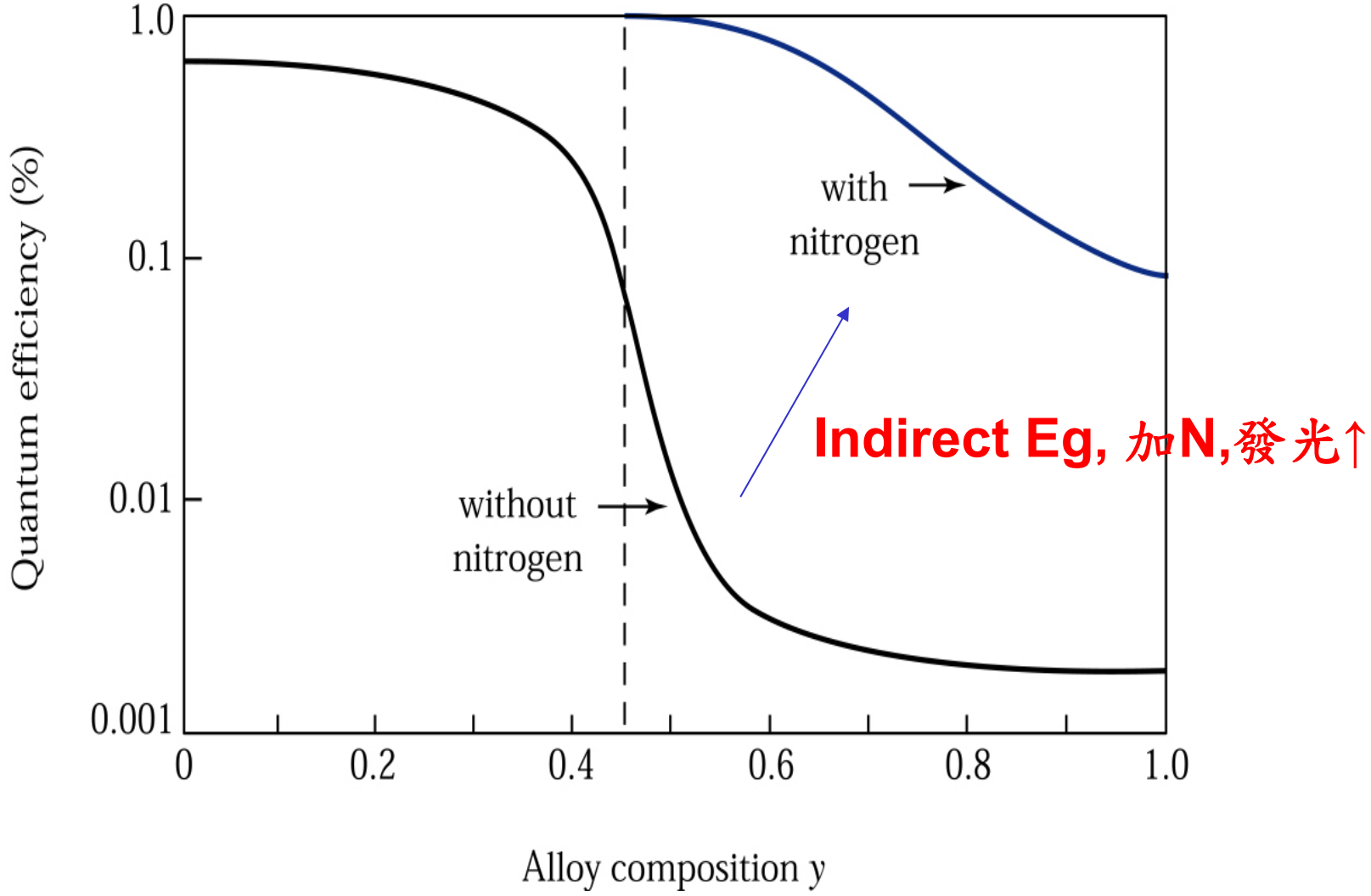

Figure 9.10b. Quantum efficiency versus alloy composition with and without isoelectronic impurity nitrogen.[4]

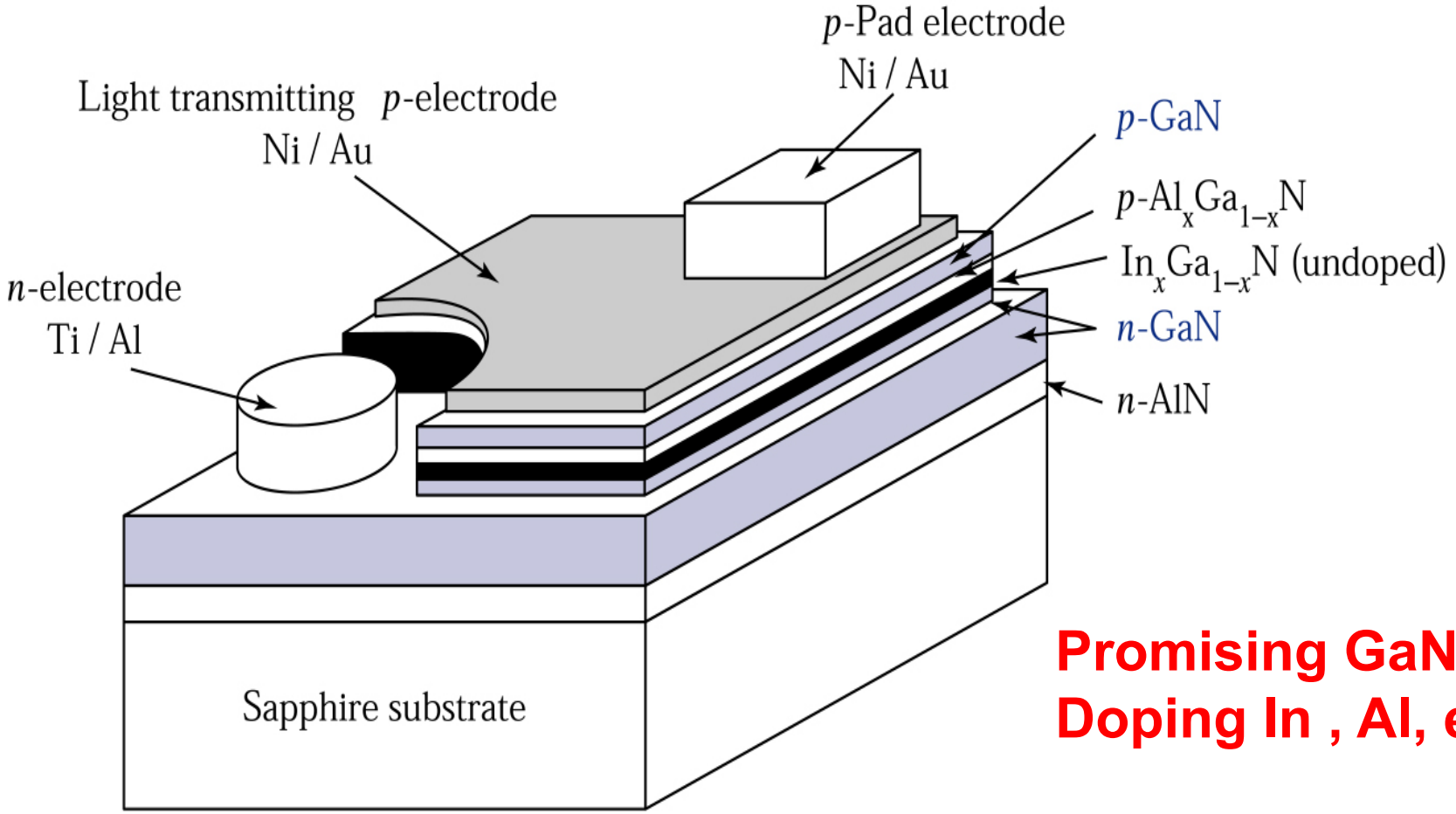

Figure 9.11a. III-V nitride LED grown on sapphire substrate.

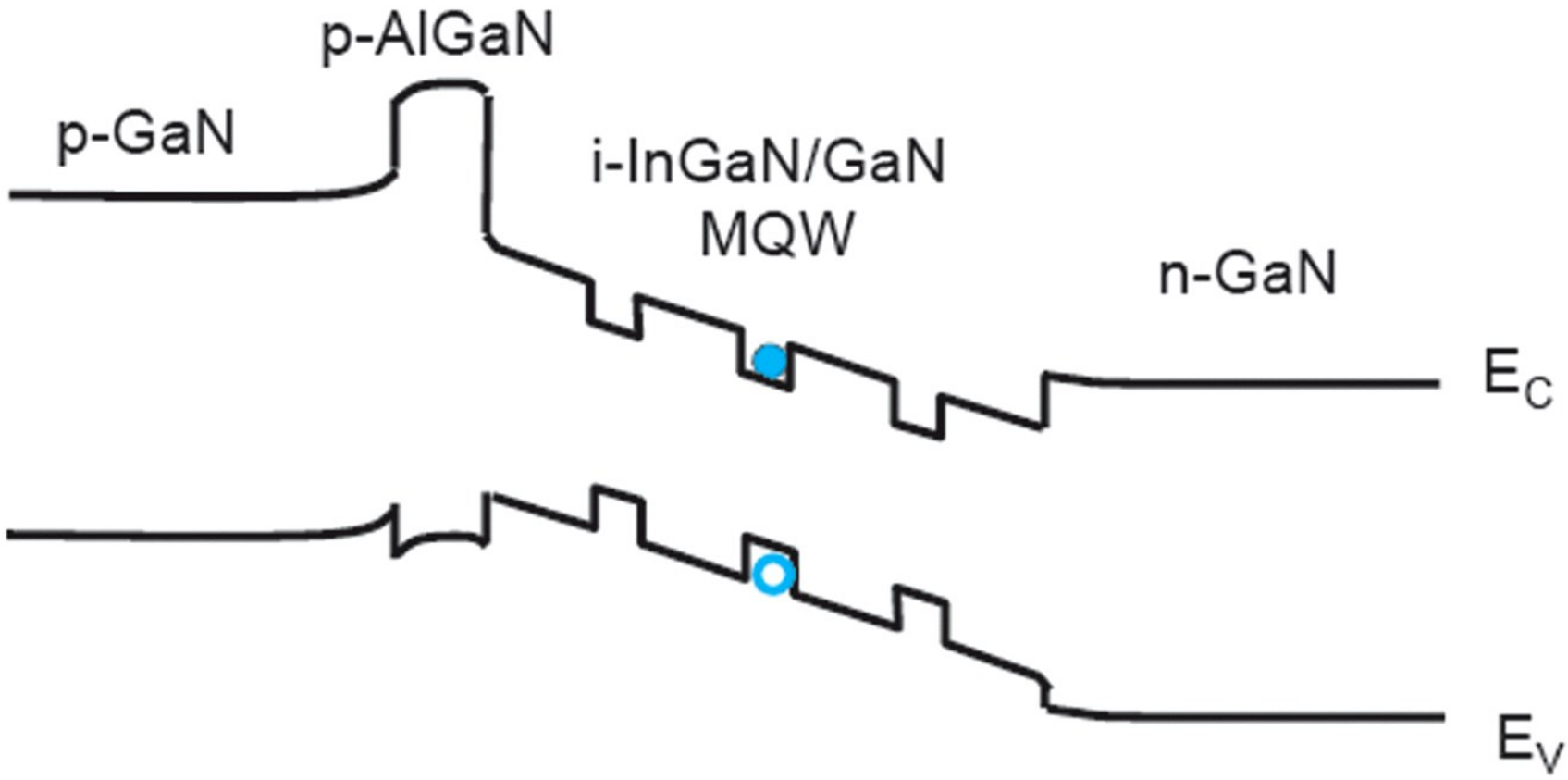

Figure 9.11b

The blue light originates from multiple quantum well (MQW)

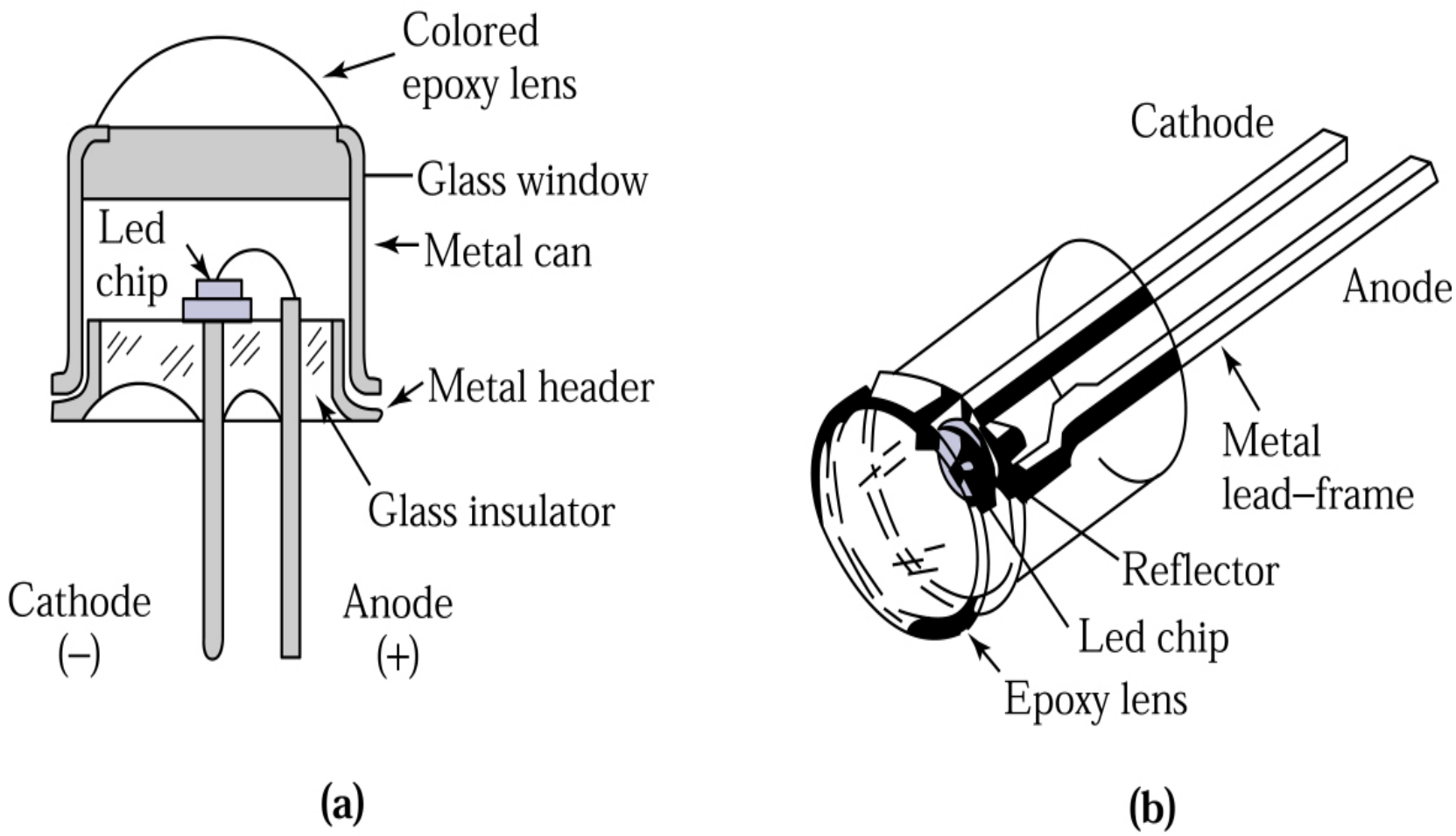

Figure 9.12. Diagrams of two LED lamps.[8]

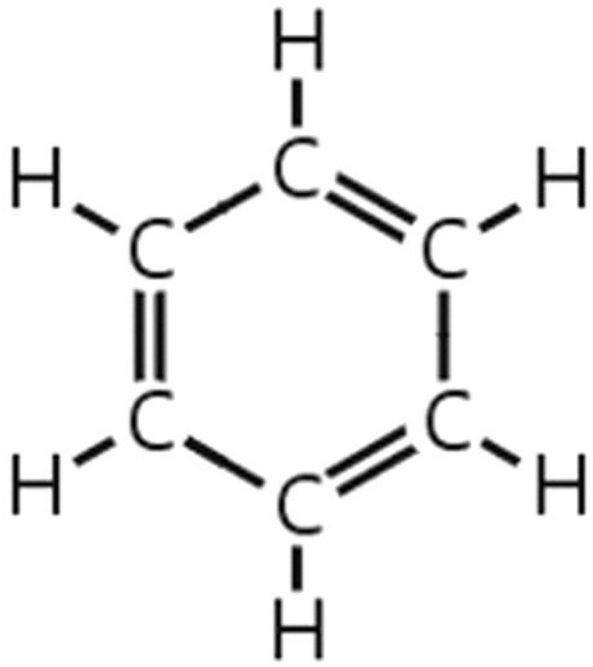

Figure 9.13

Delocalized π–bond and σ–bond of benzene

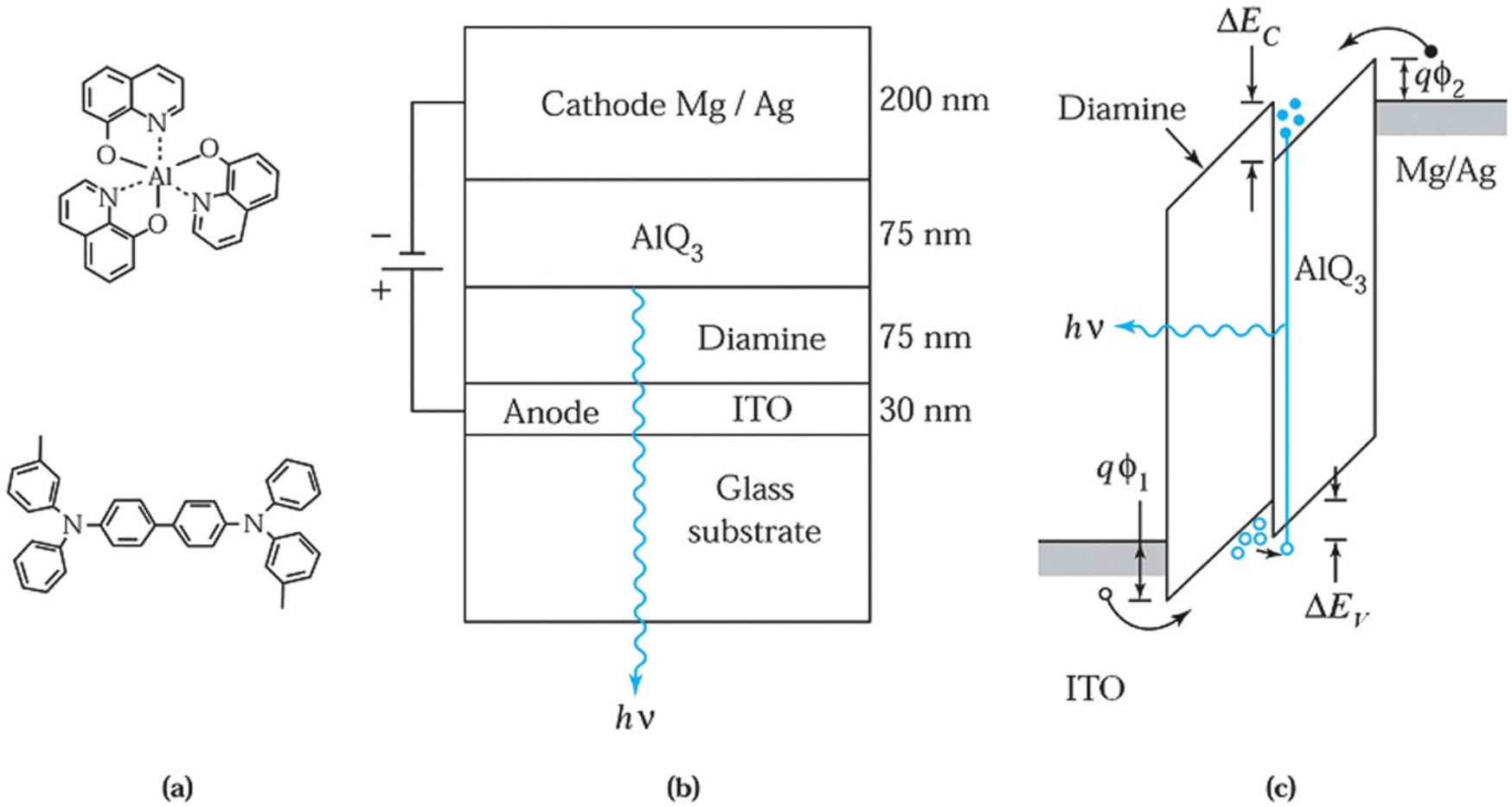

Figure 9.14

Figure 9.14. (*a*) **Organic** semiconductors. (*b*) **OLED** cross sectional view. (*c*) Band diagram of an OLED.

Large area, multi-color, wide view

OLED
(a) 3 layer

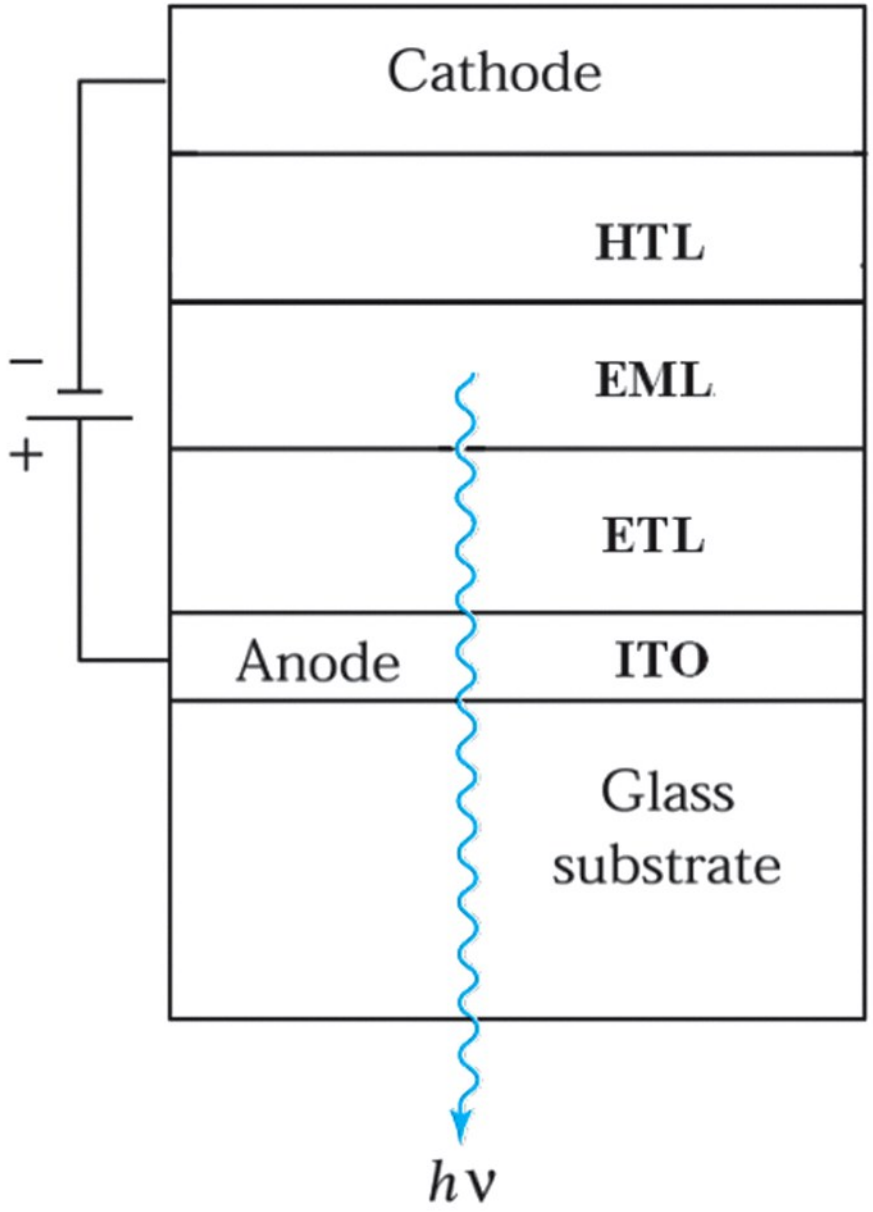

Figure 9.15a part 1

OLED
(a) 3 layer

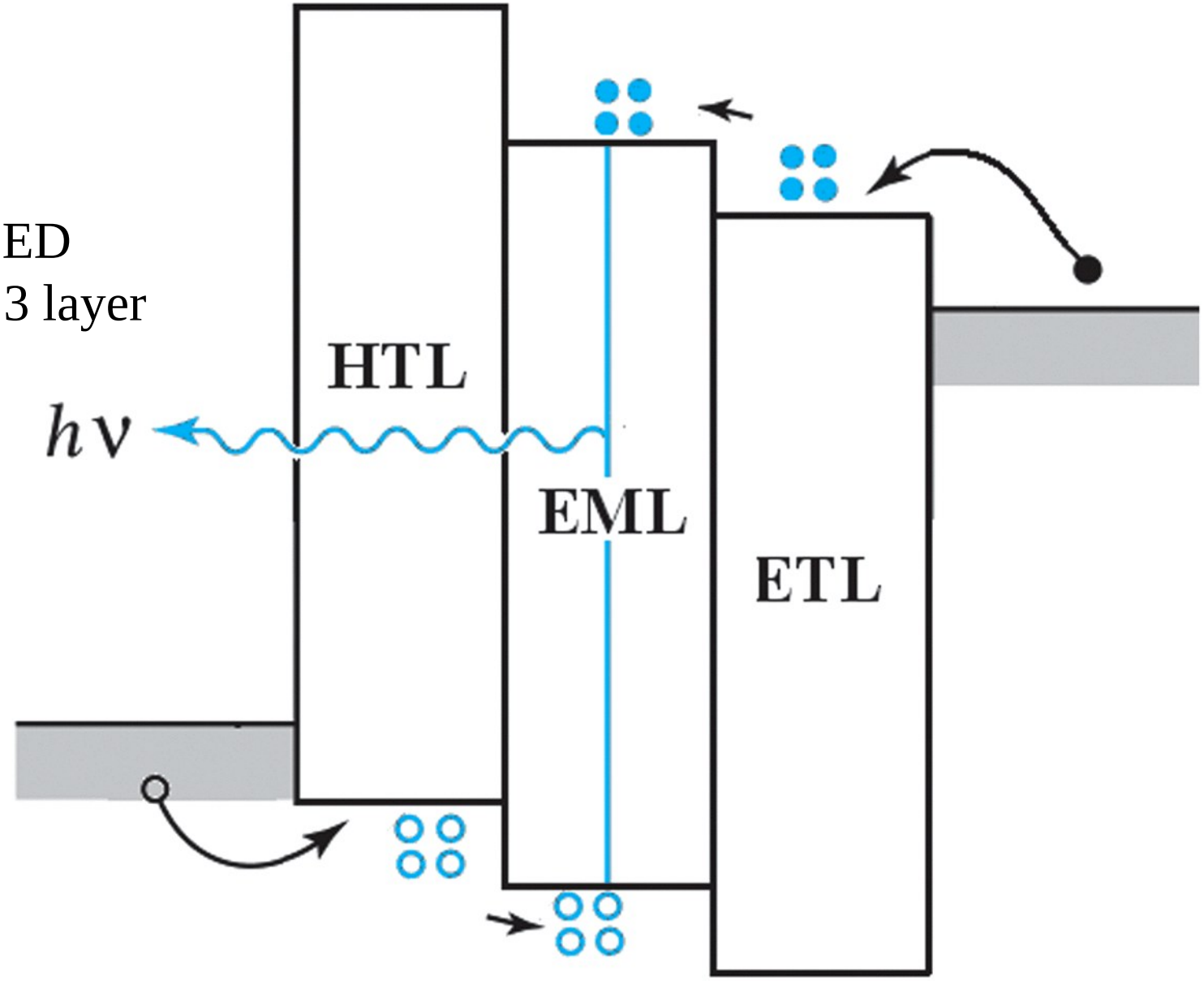

Figure 9.15a part 2

OLED
(b) 5 layer

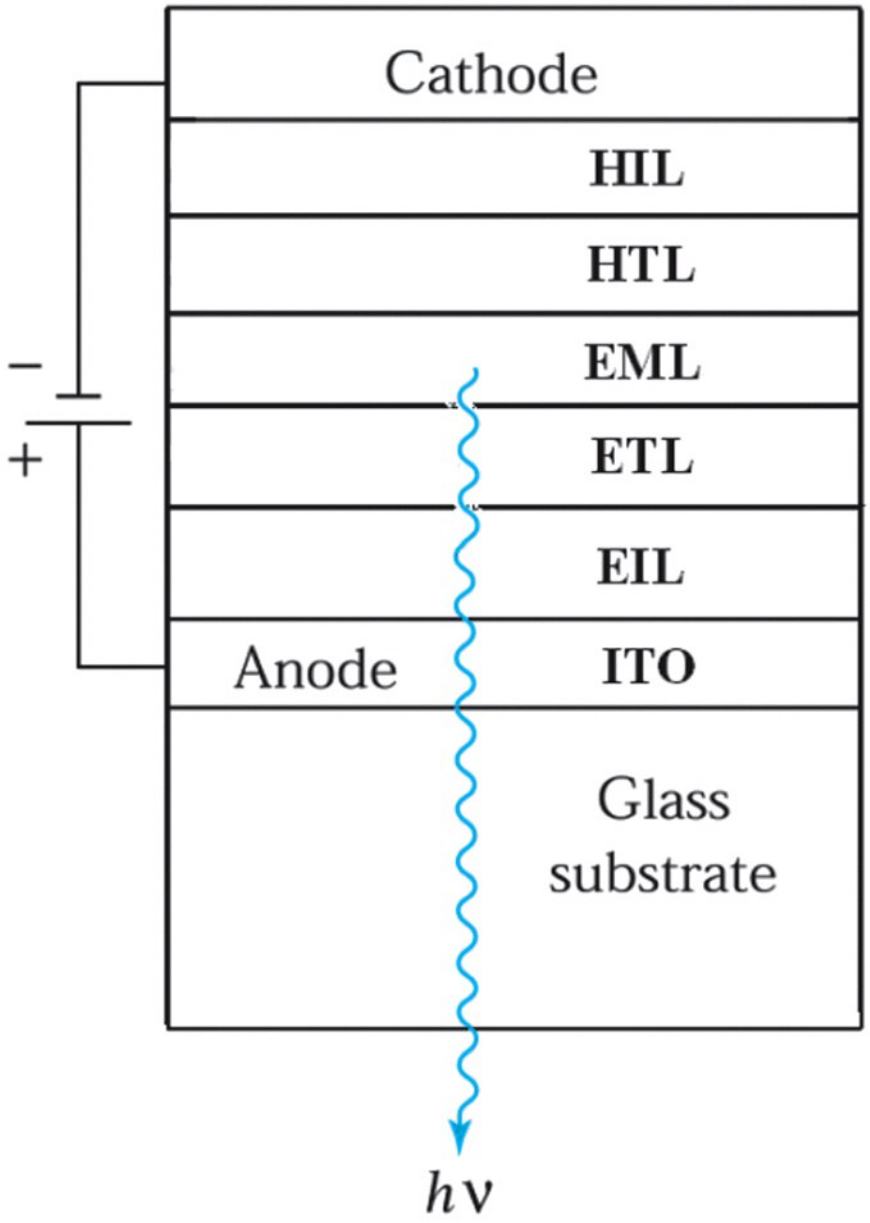

Figure 9.15b part 1

OLED
(b) 5 layer

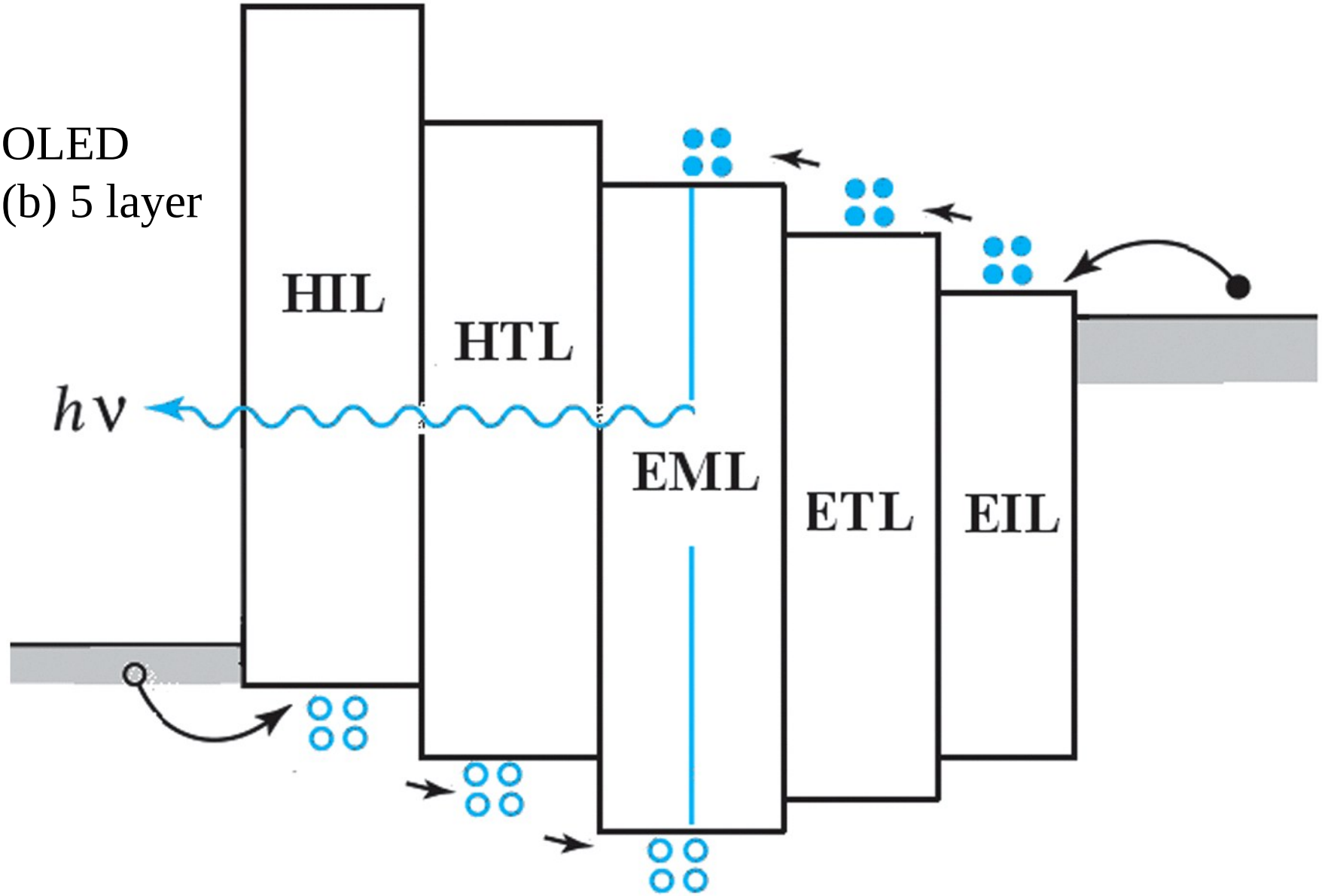

Figure 9.15b part 2

IR-LED之應用

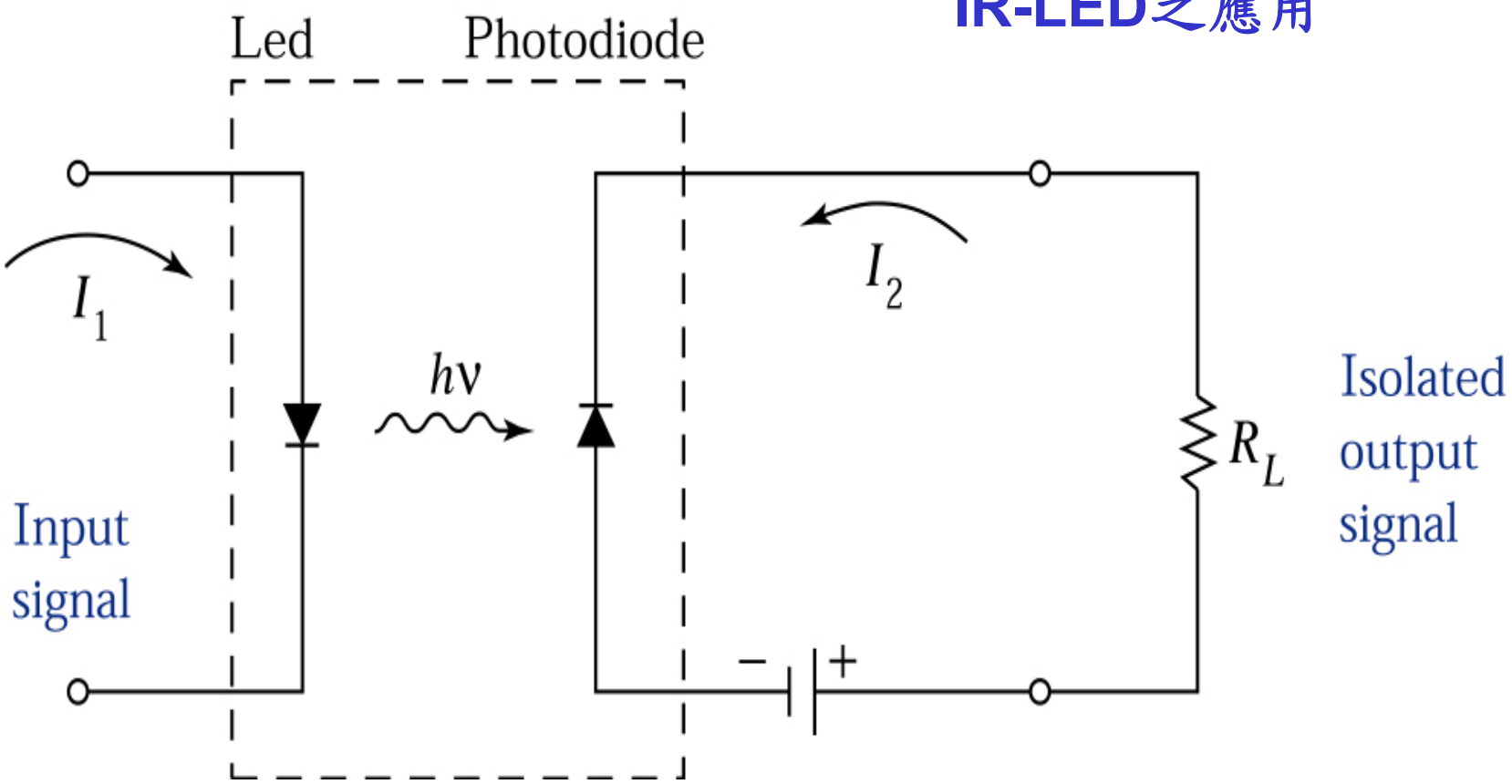

Figure 9.16. An **opto-isolator** in which an input signal is decoupled from the output signal.

Figure 9.17.
Optical fibers.
(*a*) **Step-index** fiber having a core with slightly larger reflective index.
(*b*) **Graded-index** fiber having a parabolic grading of the reflective index in the core.[11]

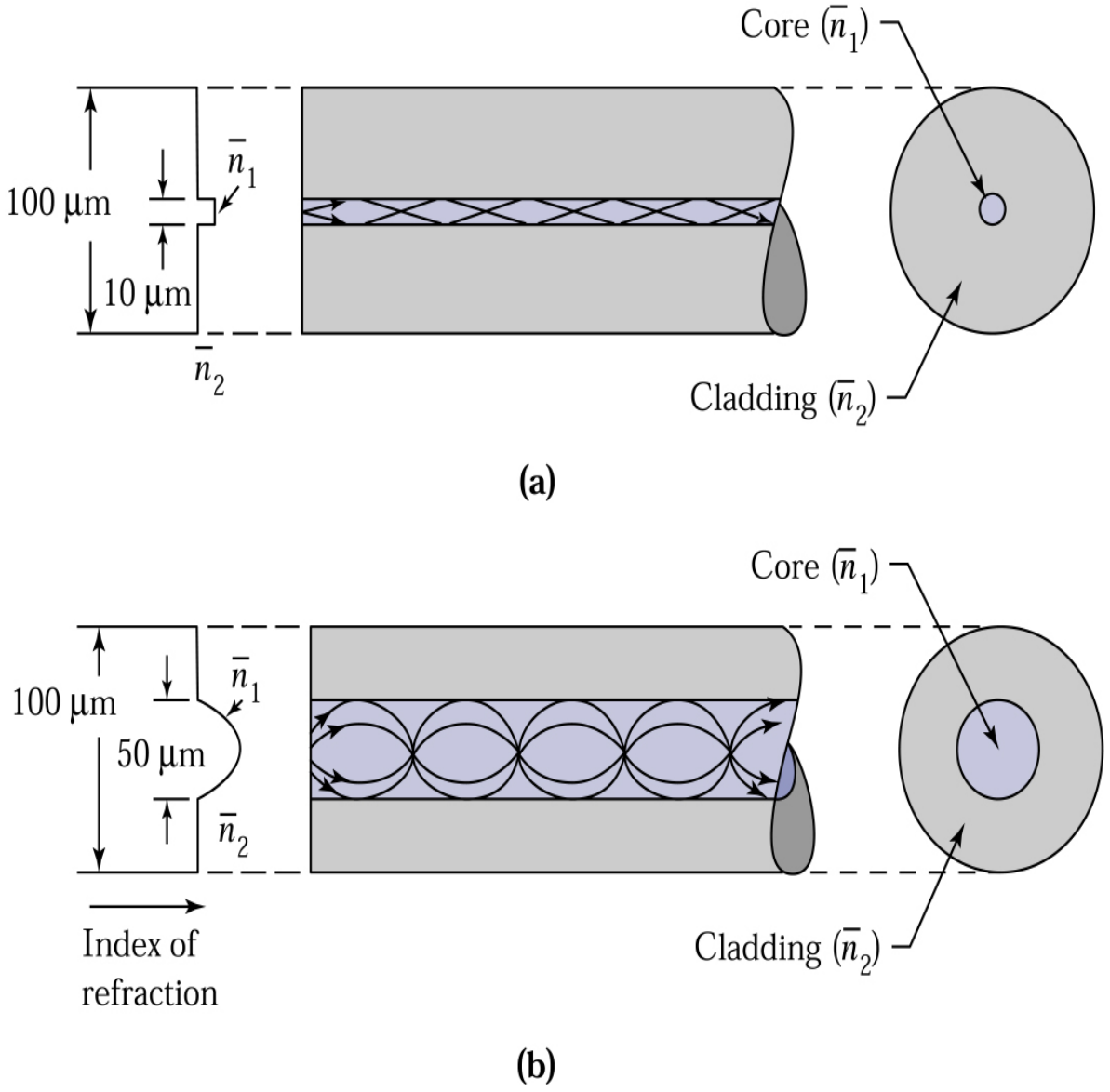

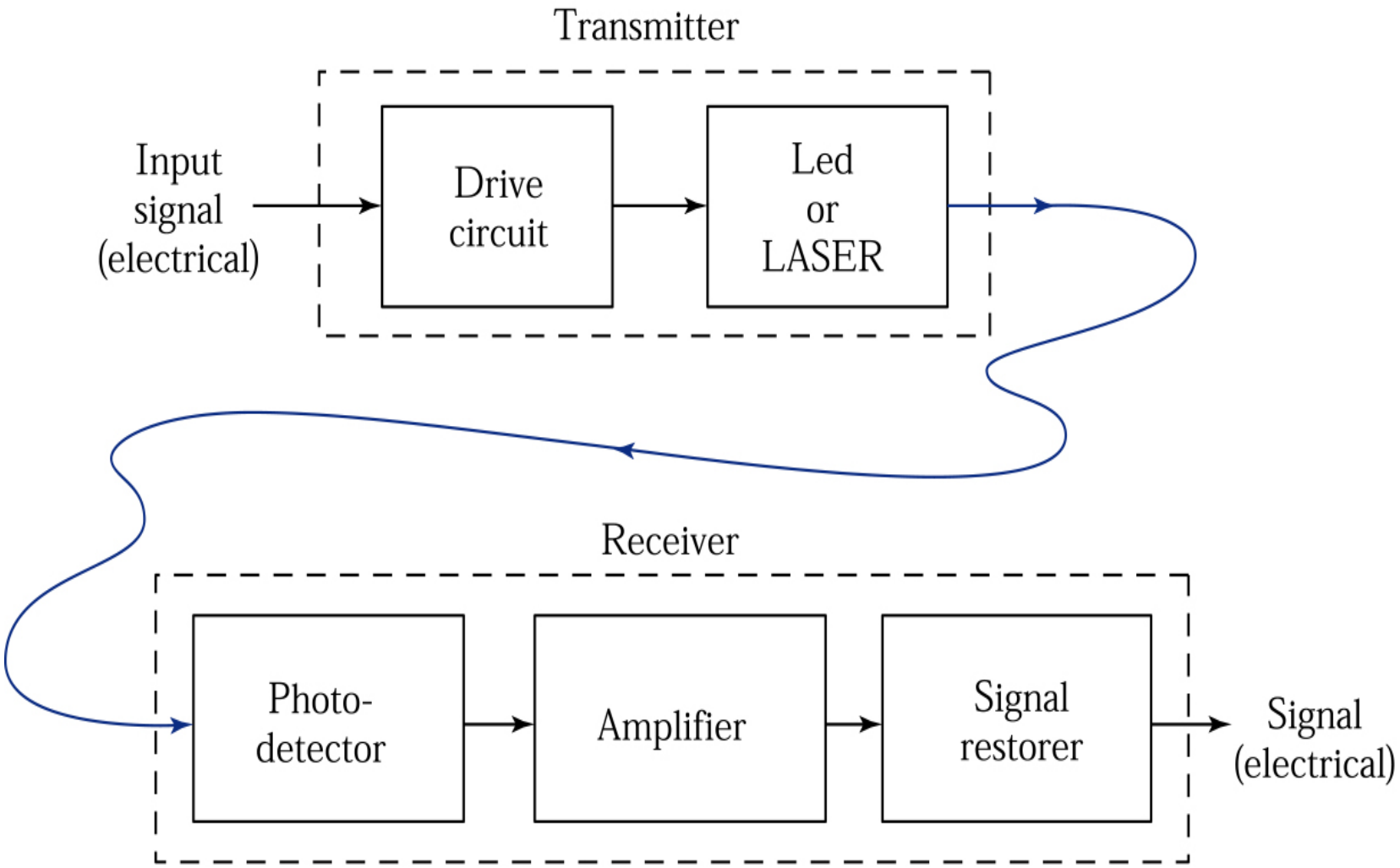

Figure 9.18. Basic elements of an optical fiber transmission link.

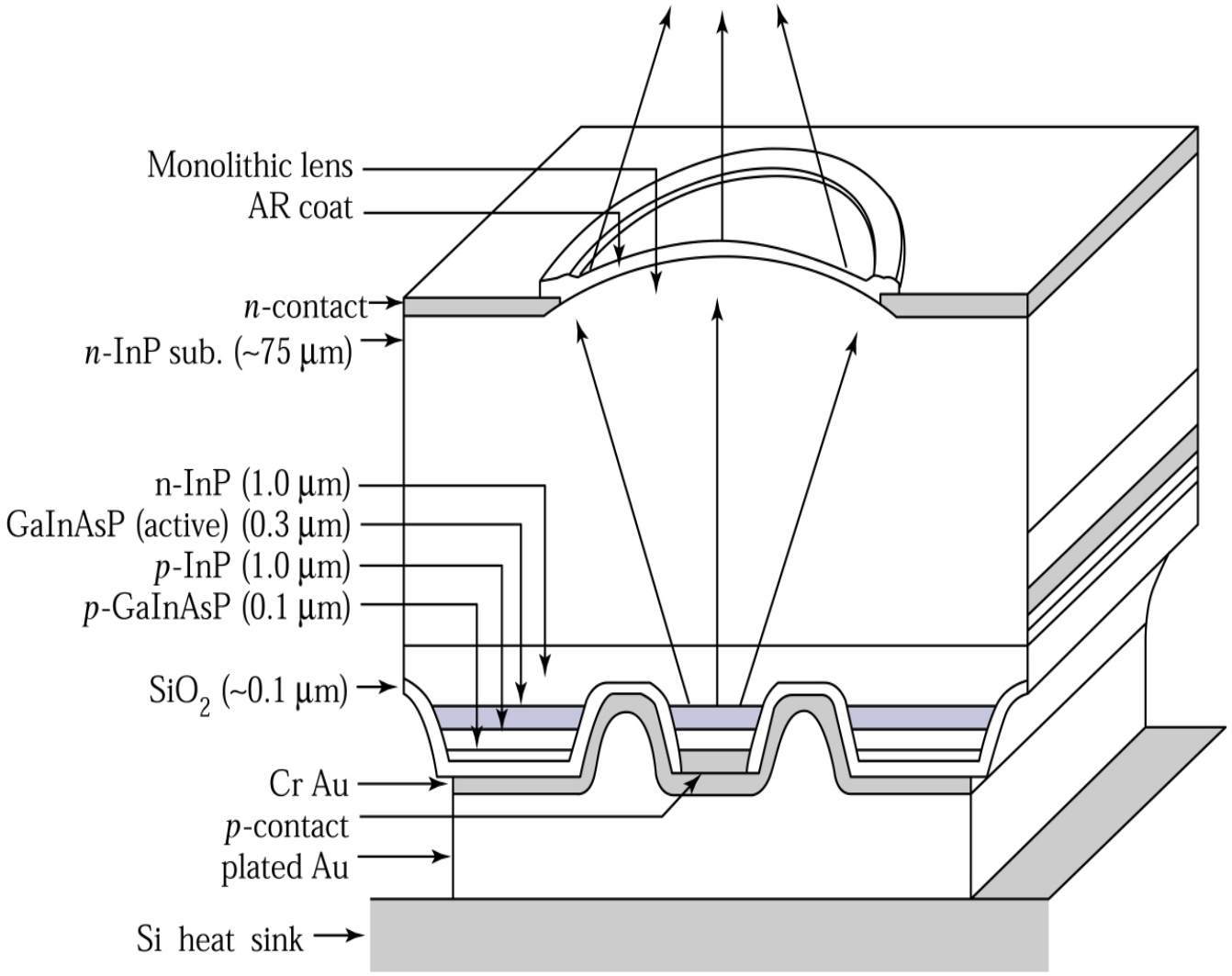

Figure 9.19. Small-area mesa-etched GaInAsP/InP surface-emitting LED structure.

Infrared LED

Figure 9.20.
Energy bandgap and lattice constant for three III-V compound solid alloy system.[13]

Laser必用direct材料

☆最重要的optical fiber 通訊光源

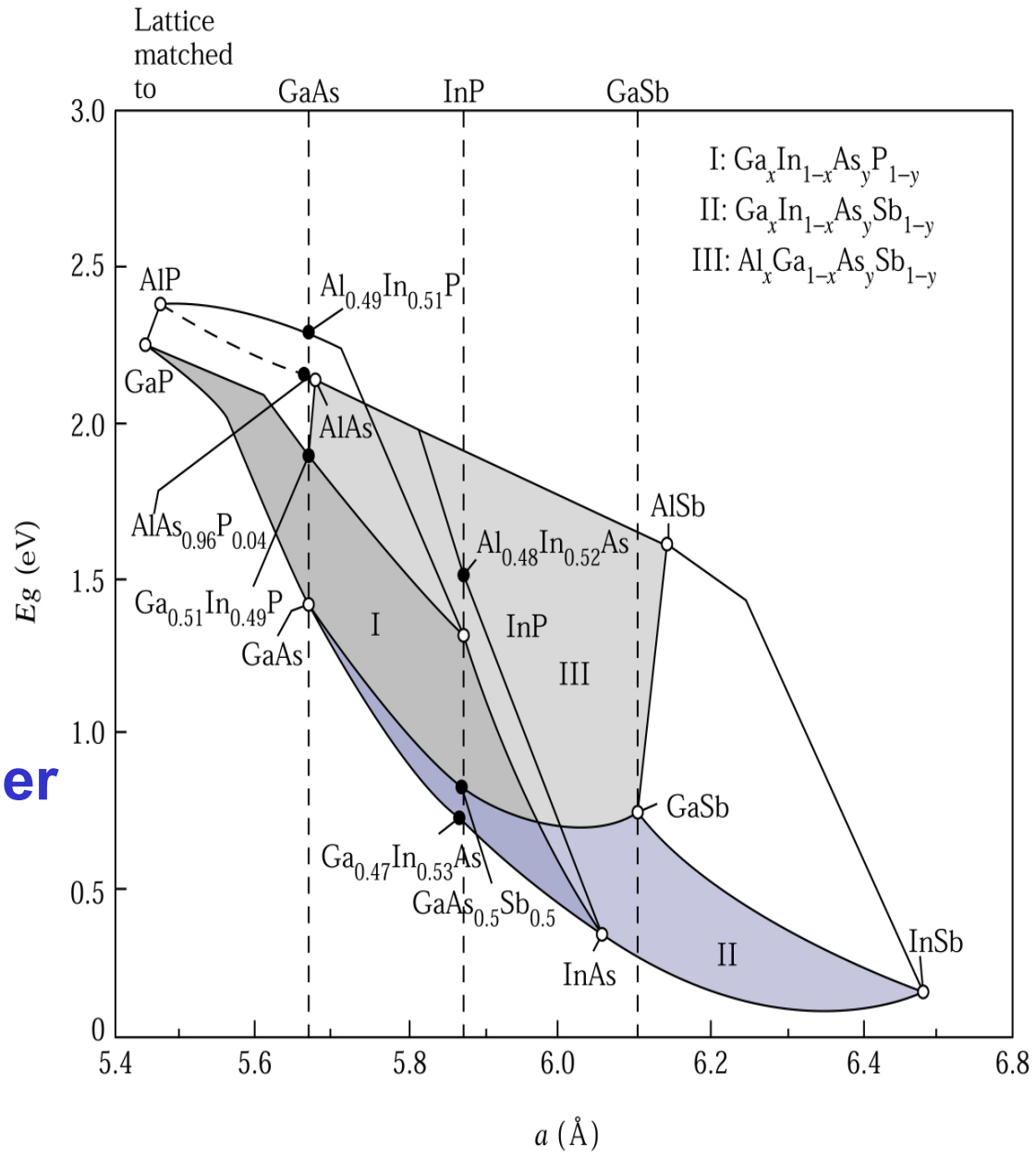

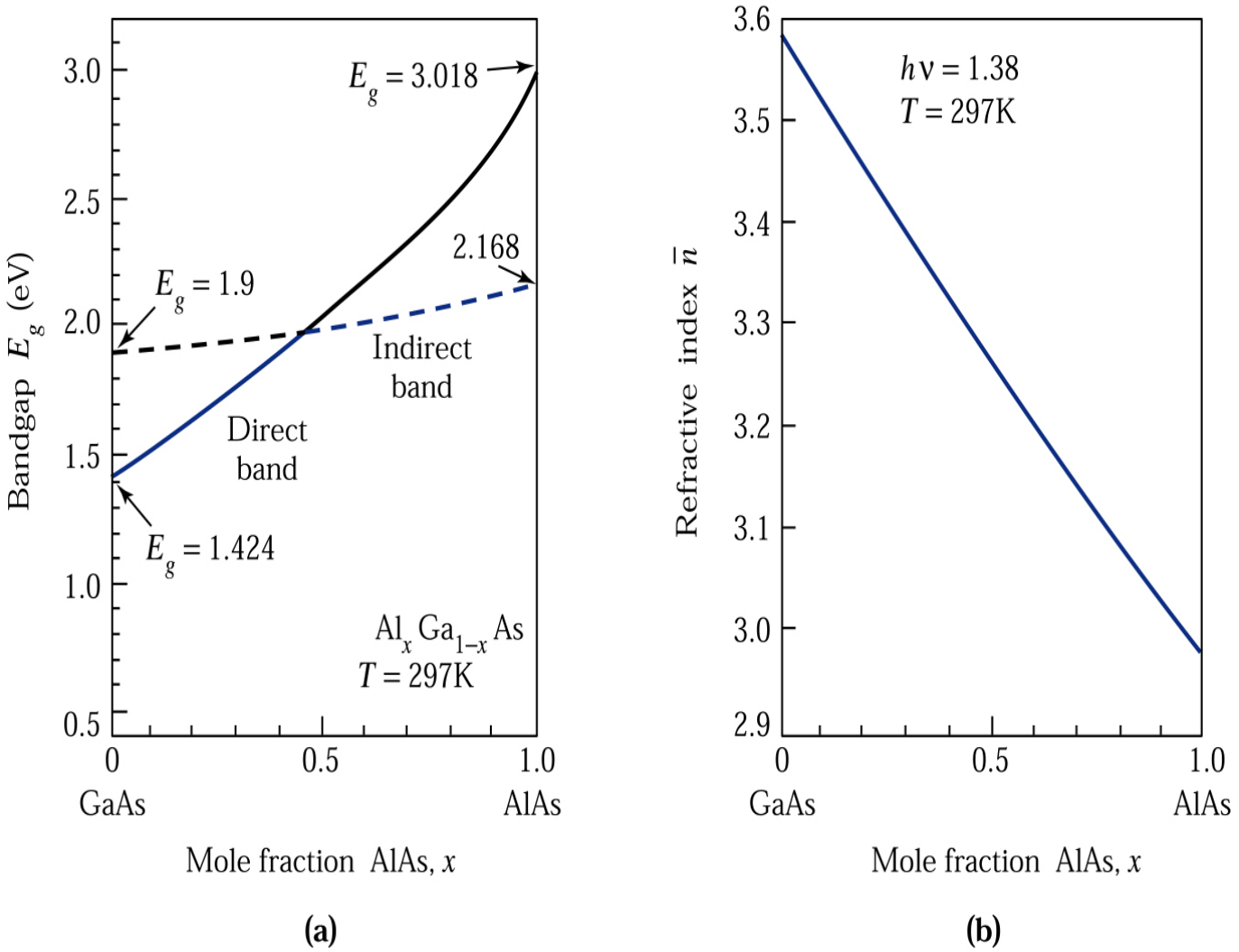

Figure 9.21. (*a*) **Compositional dependence of the $Al_xGa_{1-x}As$ energy gap.**[1] (*b*) Compositional dependence of the refractive index at 1.38 eV.

Figure 9.22. Comparison of some characteristics of (*a*) homojunction laser and (*b*) **double-heterojunction (DH)** laser. Second from the top row shows energy band diagrams under forward bias. The refractive index change for a homojunction laser is less than 1%. The refractive index change for DH laser is about 5%. The **confinement** of light is shown in the bottom row.[14]

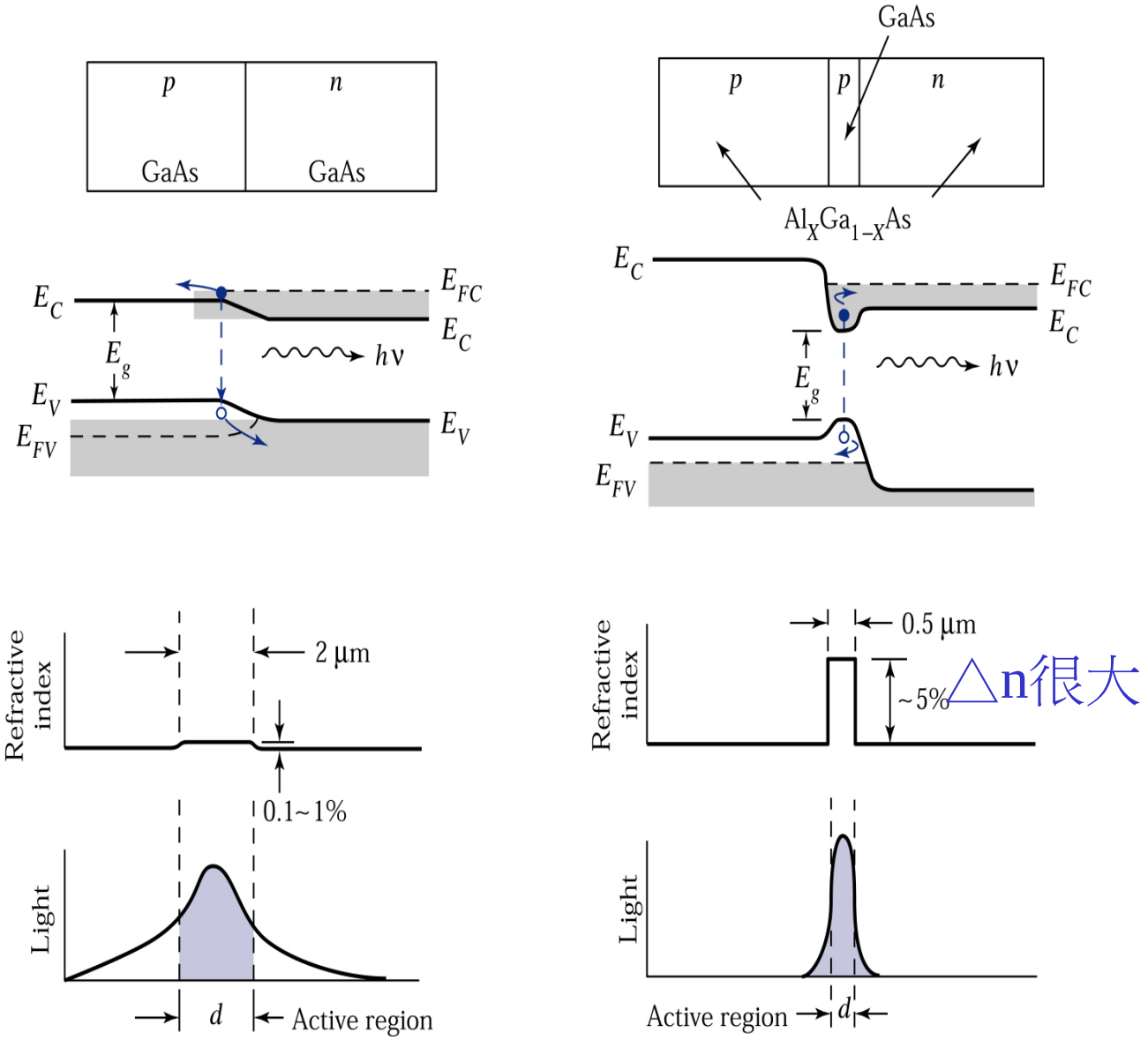

Very high doping level, population inversion

confinement

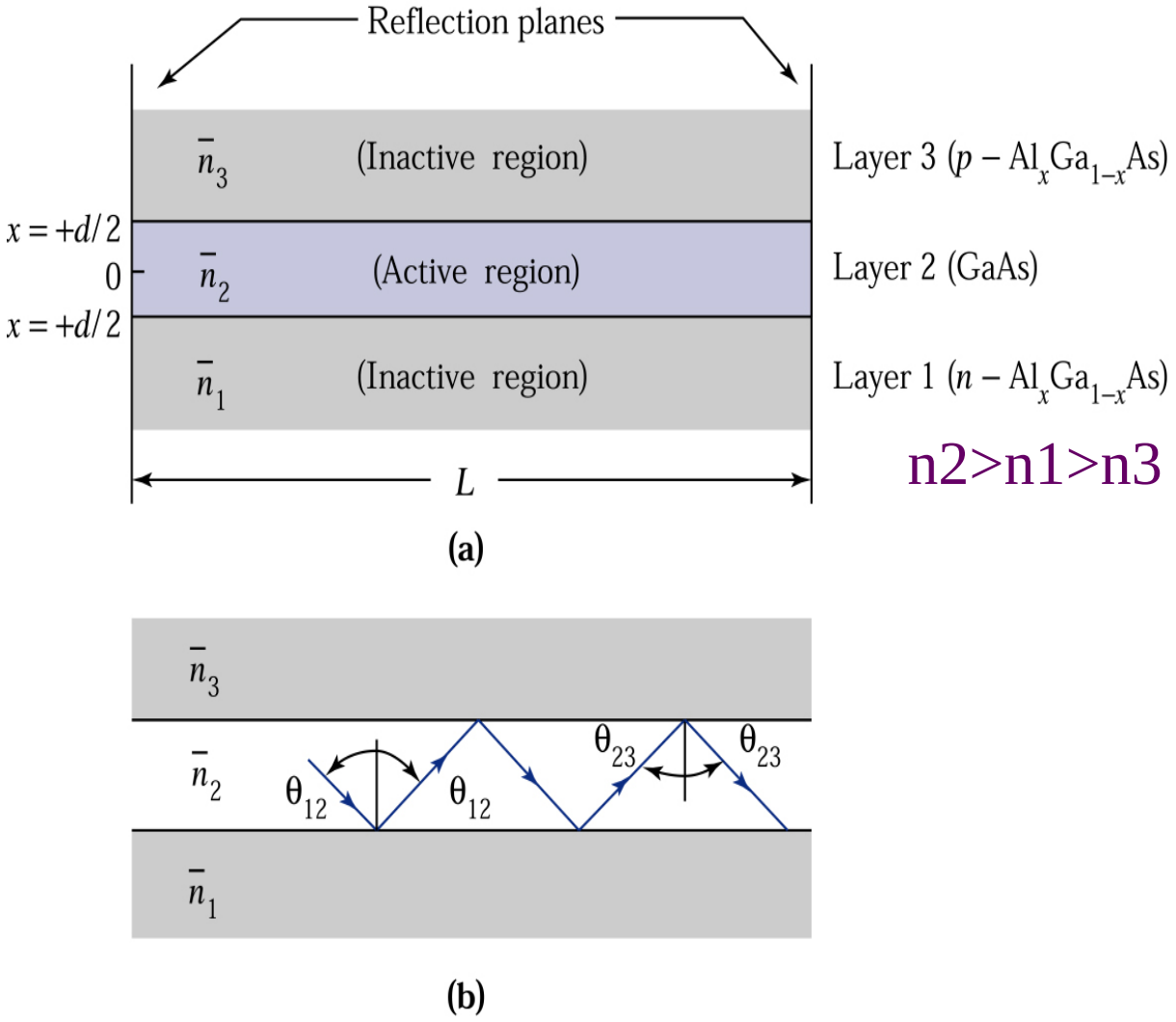

Figure 9.23. (*a*) Representation of a three-layer dielectric waveguide. (*b*) Ray trajectories of the guided wave.

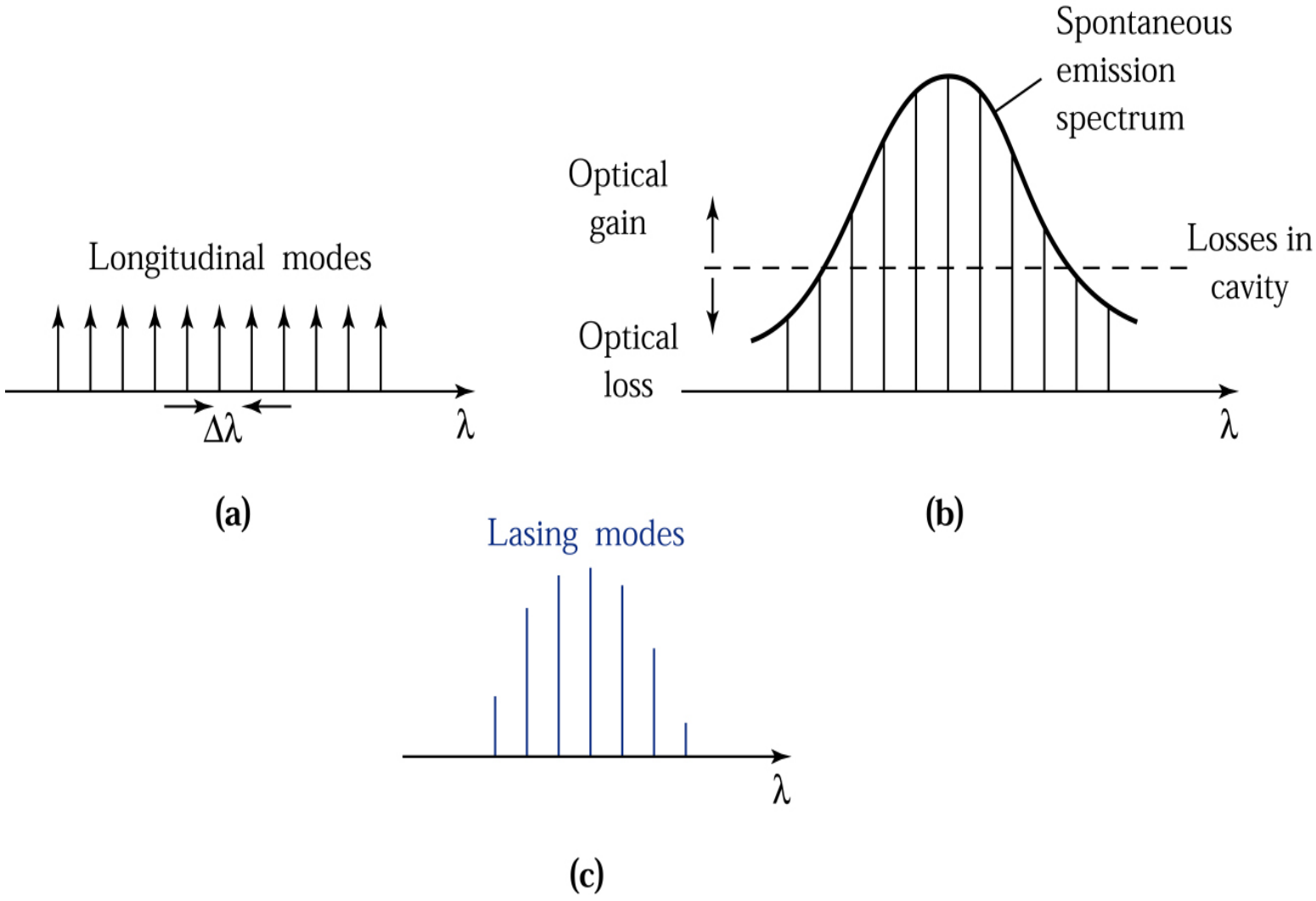

Figure 9.24. (*a*) Resonant modes of a laser cavity. (*b*) Spontaneous emission spectrum. (*c*) Optical-gain wavelengths.

Figure 9.25.
Semiconductor laser structure in the Fabry-Perot-cavity configuration. (*a*) Homojunction laser. (*b*) Double-heterojunction (DH) laser. (*c*) **Stripe-geometry DH laser.**[14,15]

很粗糙
使光不放出

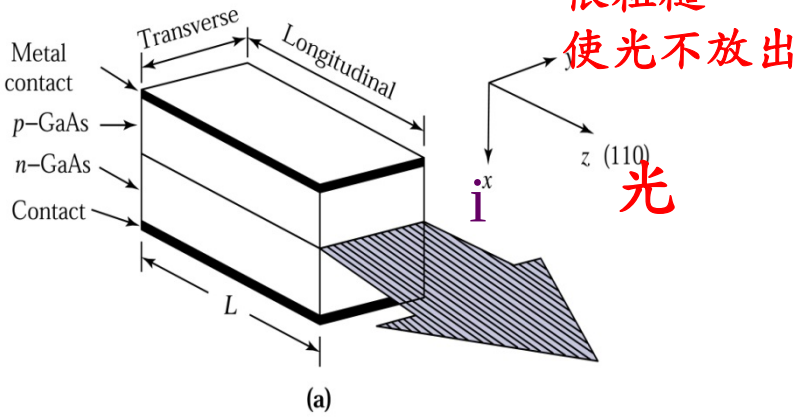

上下 **confinement**

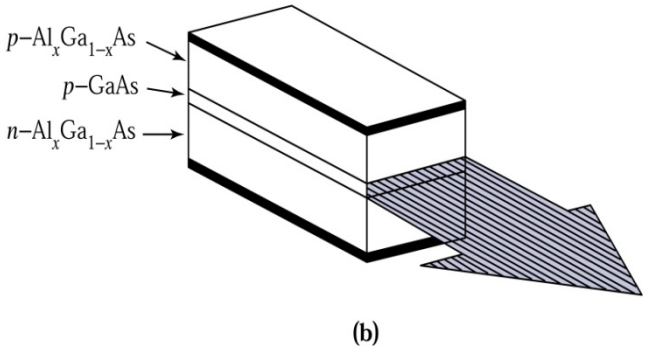

上下左右 **confinement**

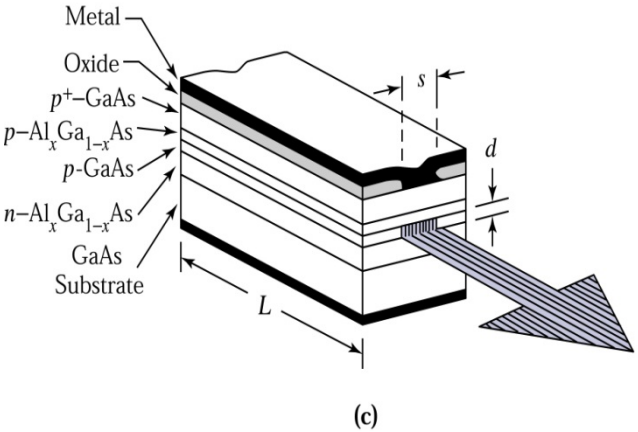

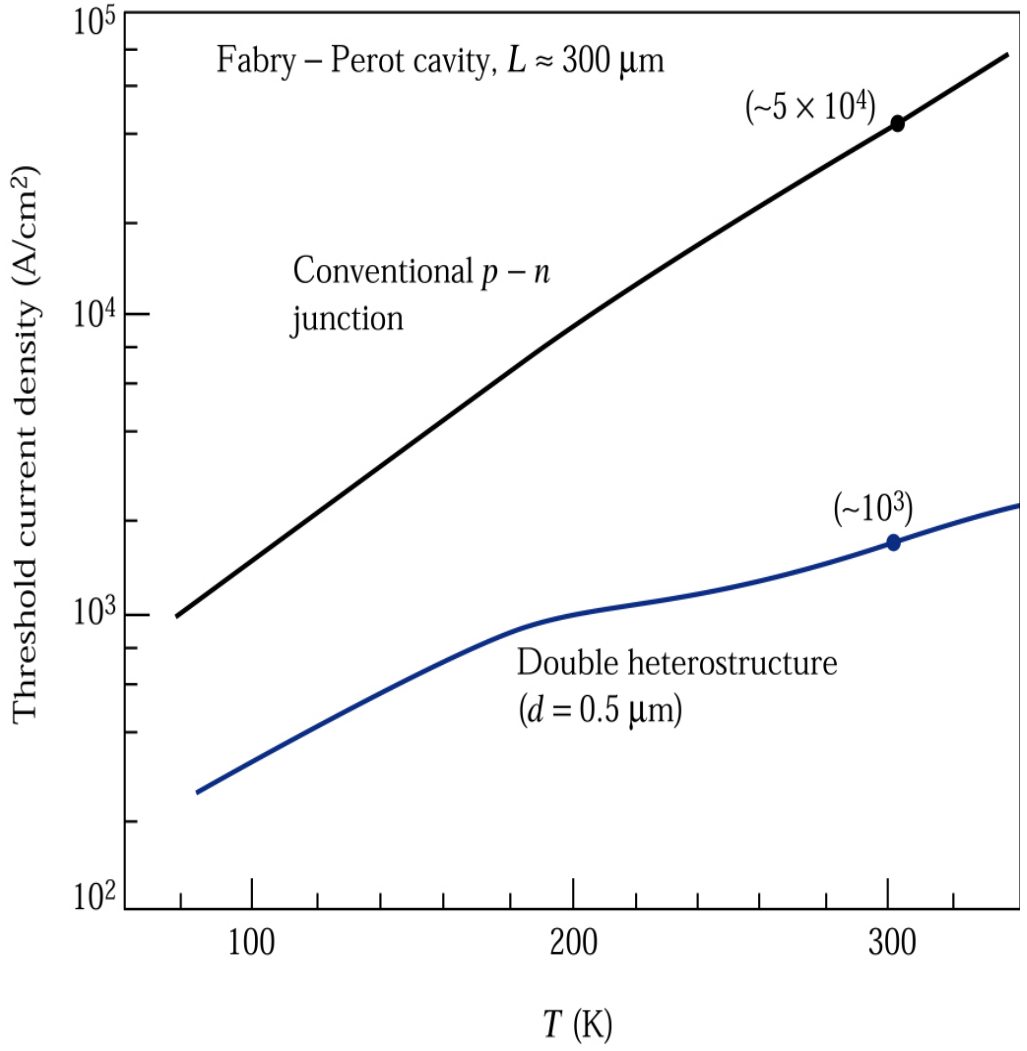

Temp ↑, I_{th} ↑

DH, I_{th} ↓

Figure 9.26. **Threshold current density** versus temperature for the two laser structures shown[14] in Fig. 9-20.

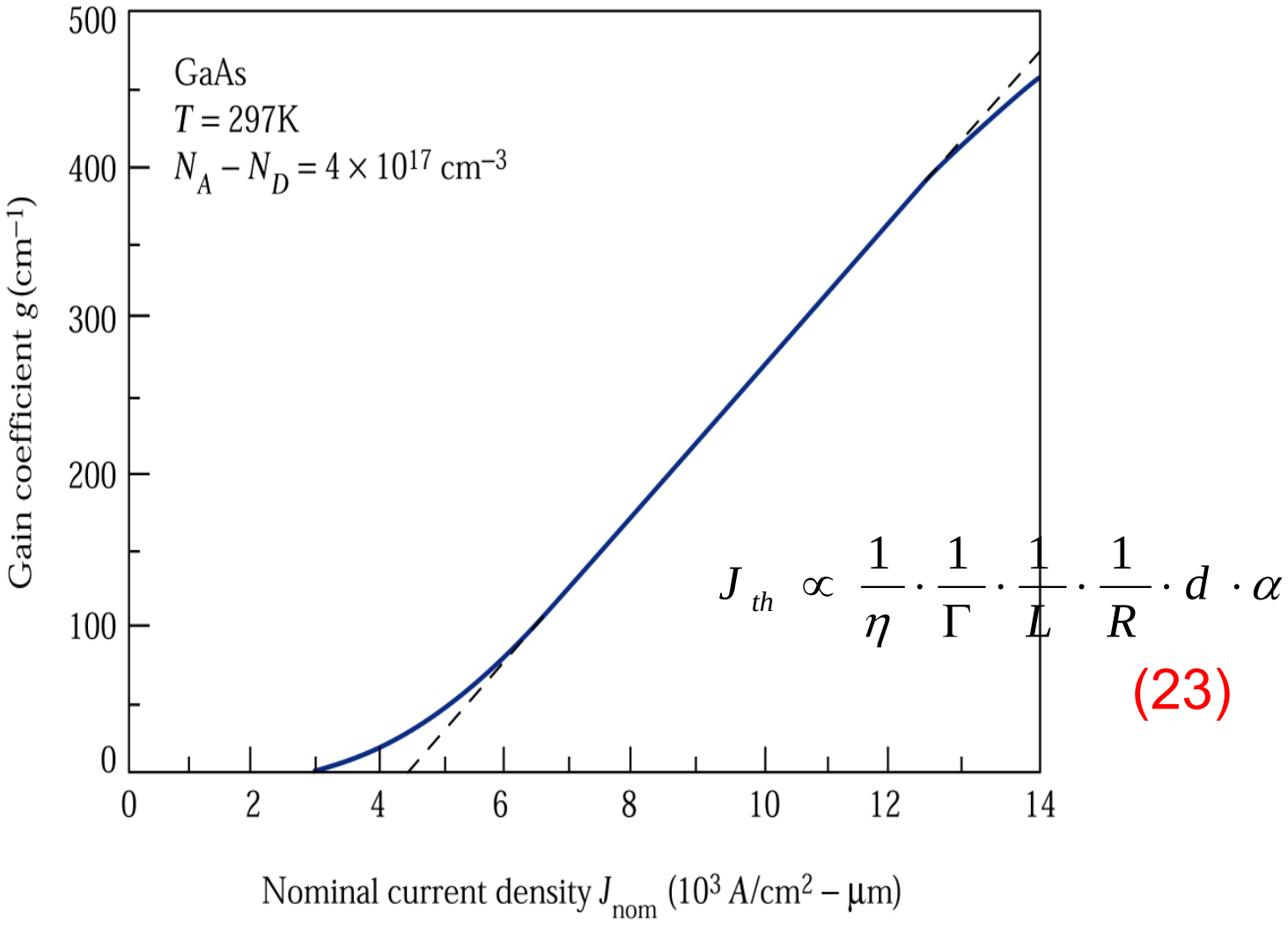

Figure 9.27. Variation of gain coefficient versus nominal current density. Dashed line represents a linear dependence.[16]

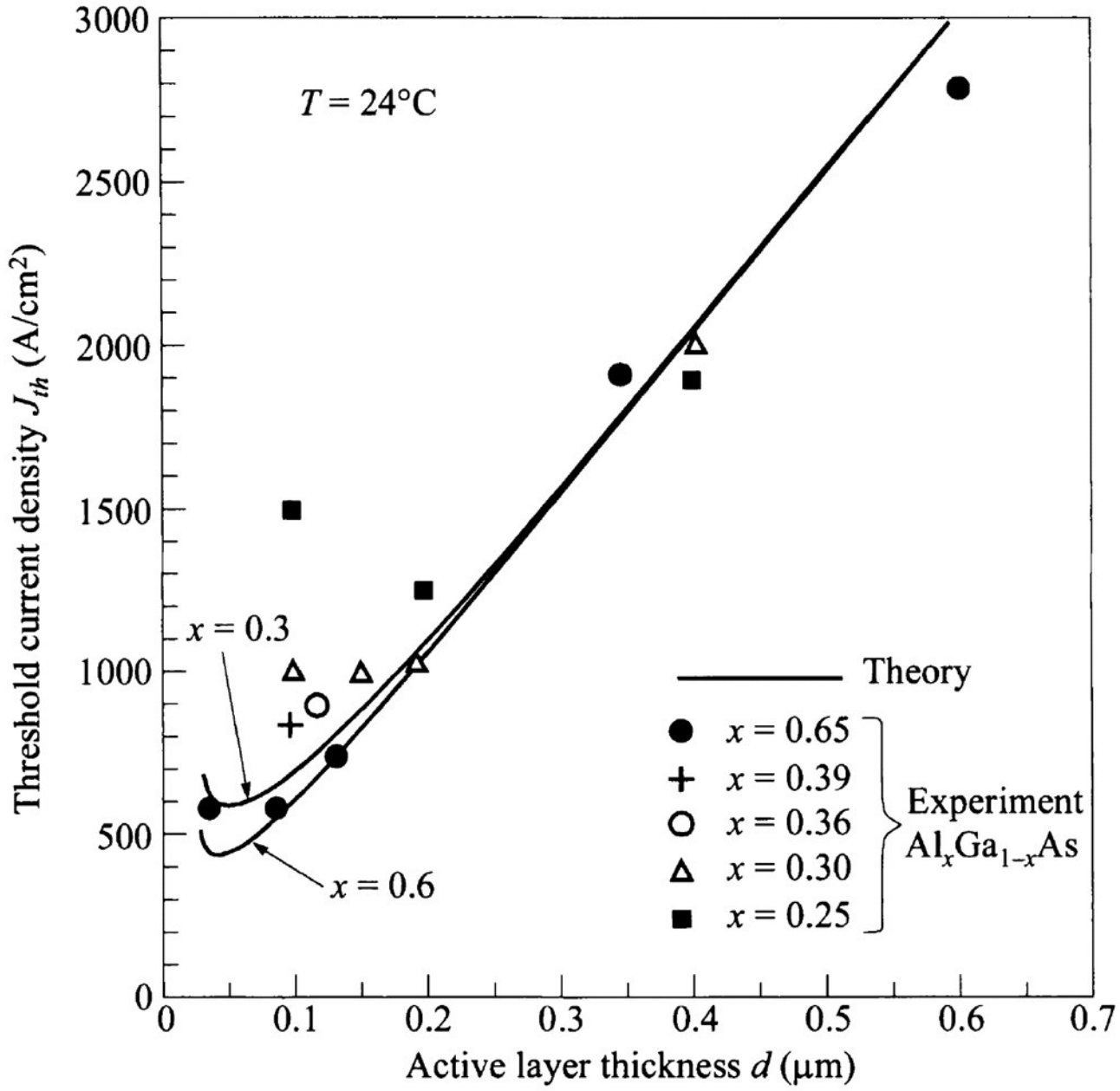

Figure 9.28

Figure 9.29.
(a) **Light output versus diode current** for a GaAs/AlGaAs heterostructure laser.
(b) Temperature dependence of the continuous wave (cw)-current threshold.[17]

Temp↑, Ith↑

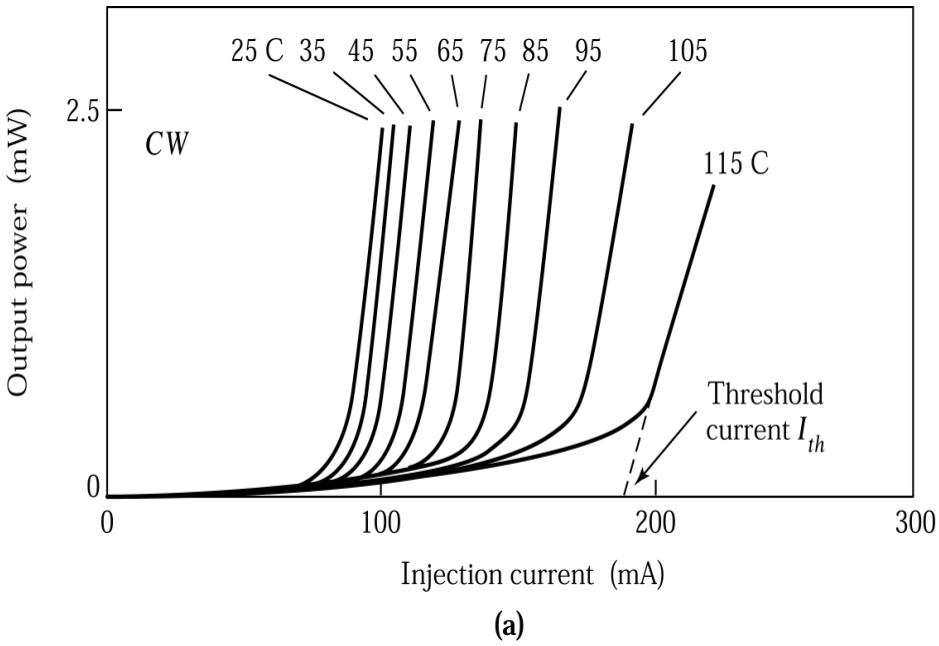

(a)

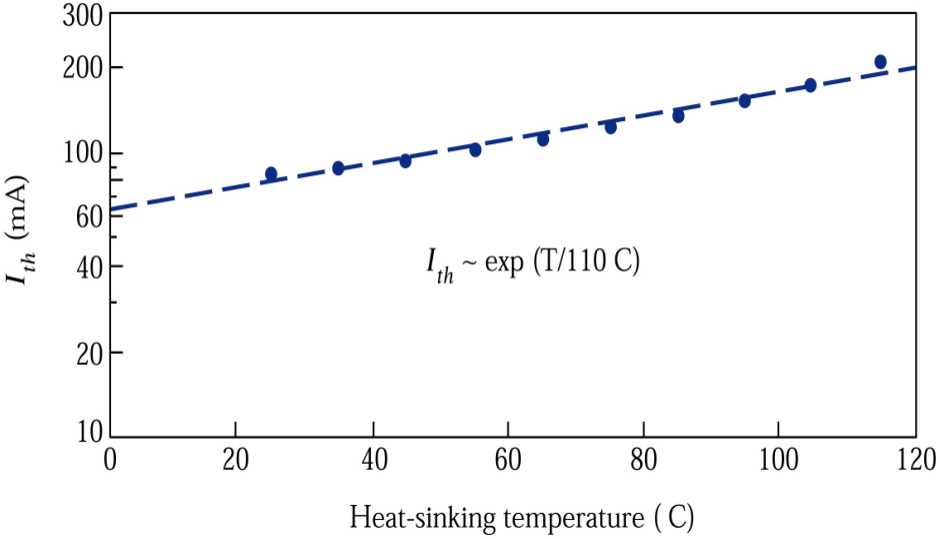

(b)

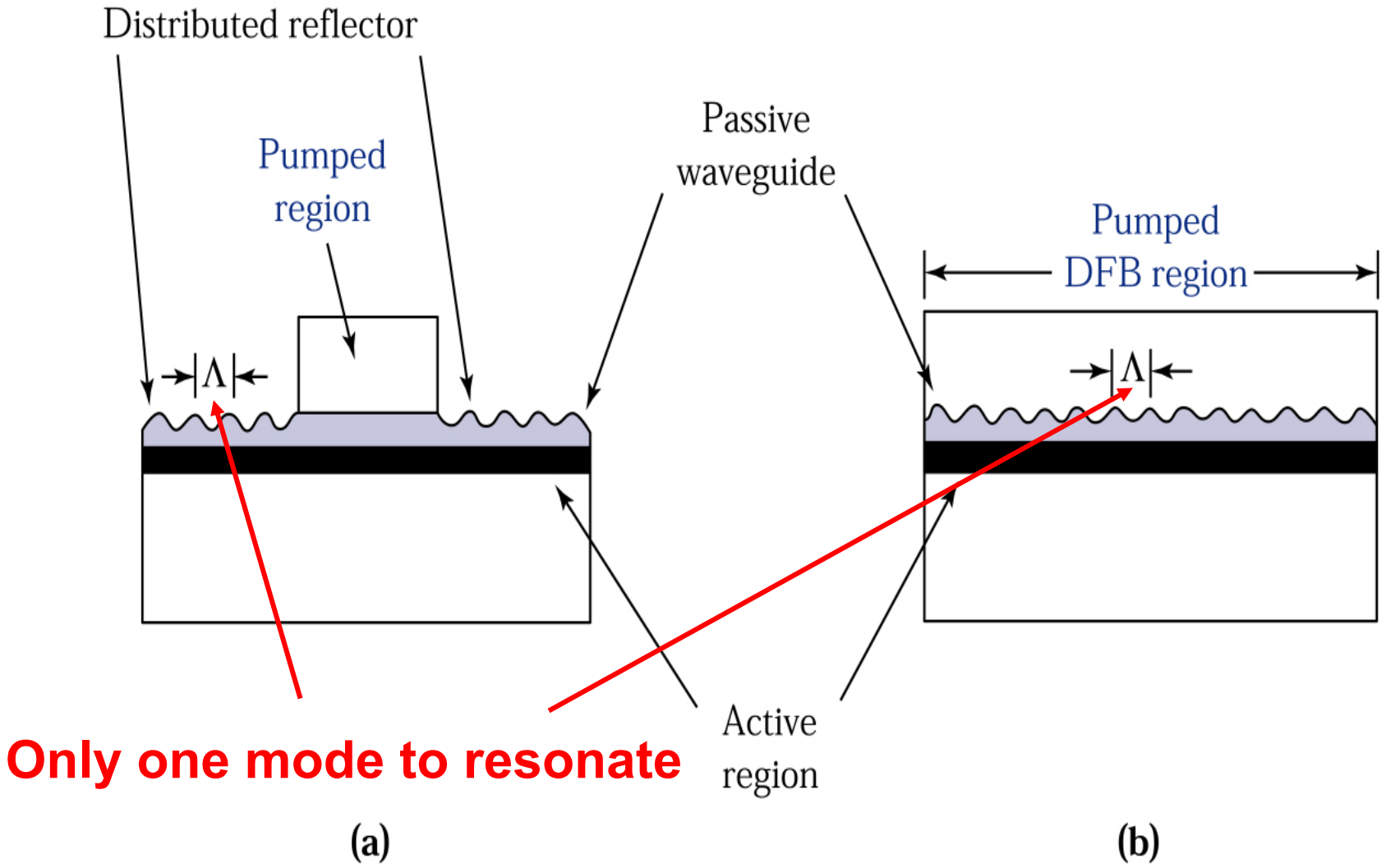

Figure 9.30. Two methods of obtaining a **single-frequency laser**. (*a*) Distributed Bragg reflector (DBR) laser, and (*b*) a distributed feedback (DFB) laser.

Figure 9.31.
The **quantum-well (QW) laser:**
(*a*) single GaAs QW surrounded by AlGaAs, (*b*) discrete energy levels within the well, and
(*c*) density of states for electrons and holes within the well.
(d) electron concentration distribution

Similar to DH,
Active layer ~10-20 nm,
Ith ↓

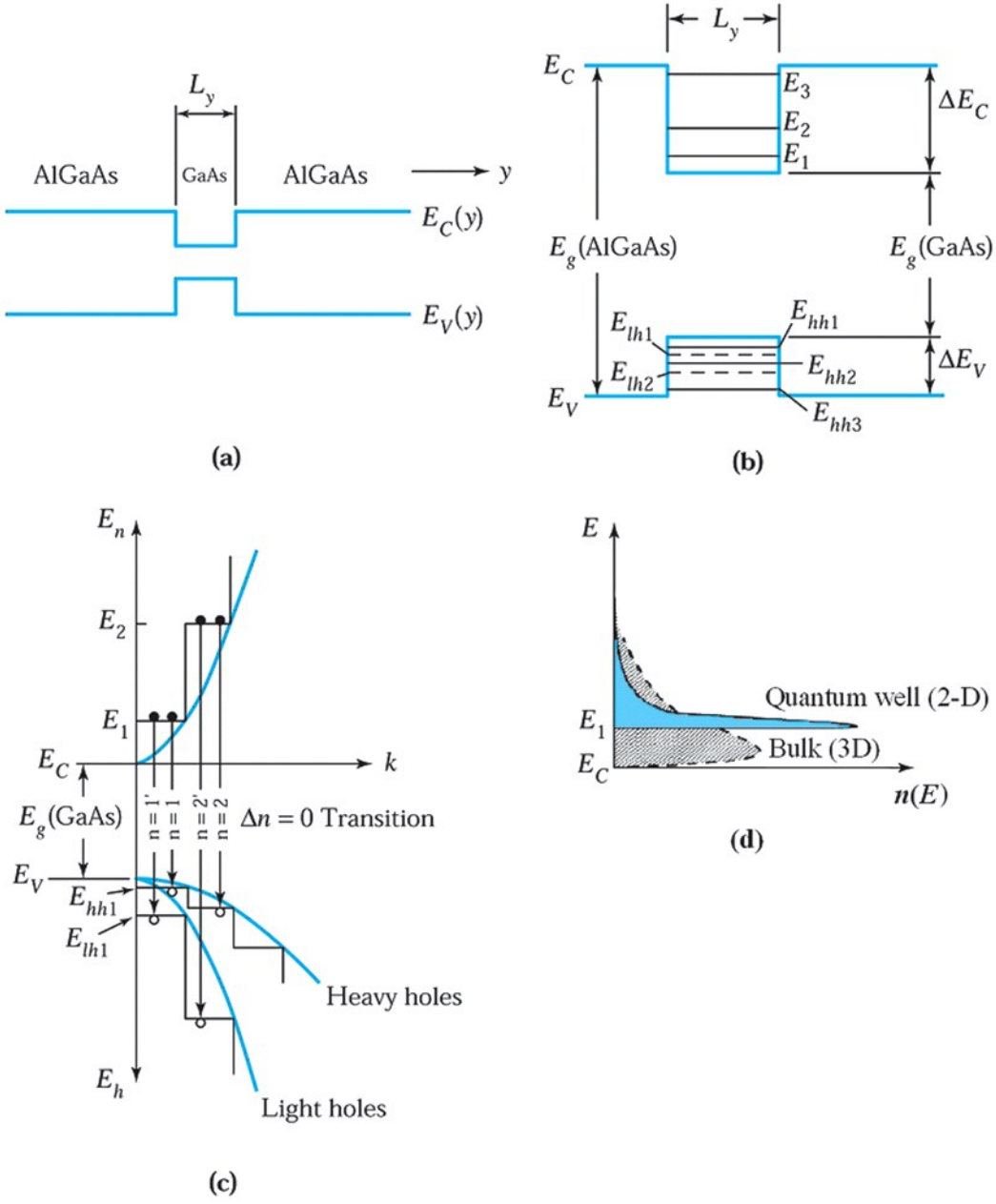

Figure 9.31

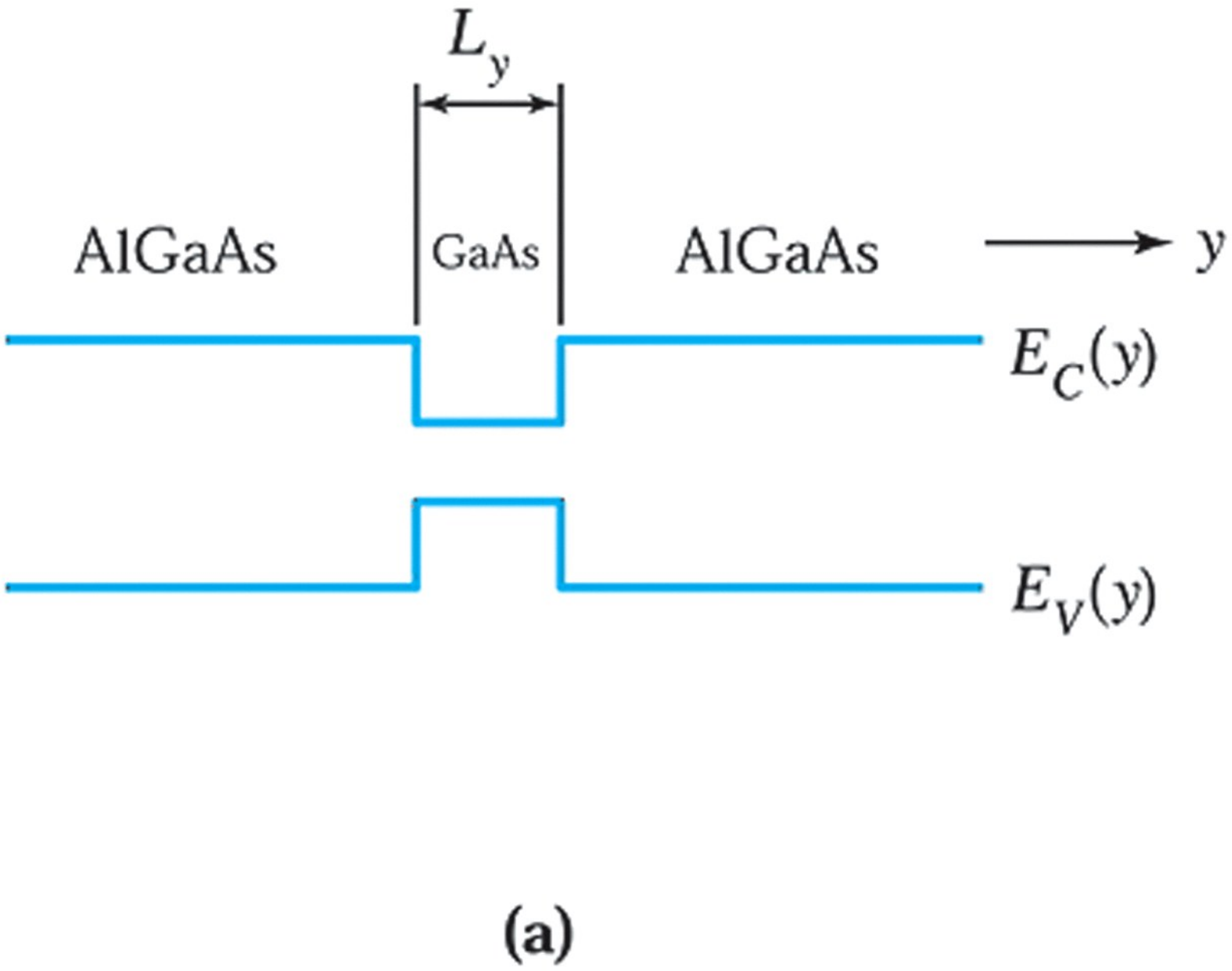

Figure 9.31a

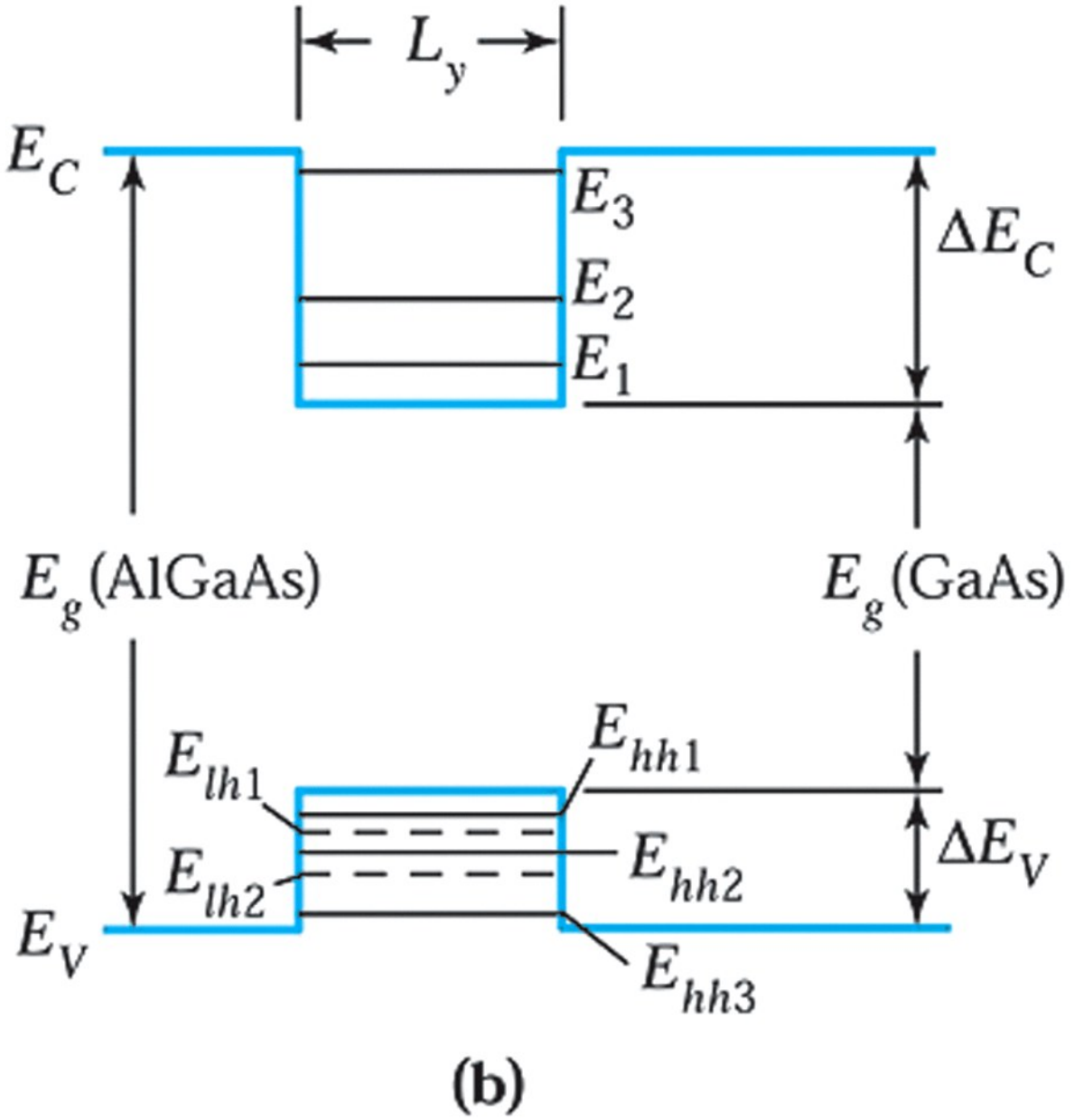

Figure 9.31b

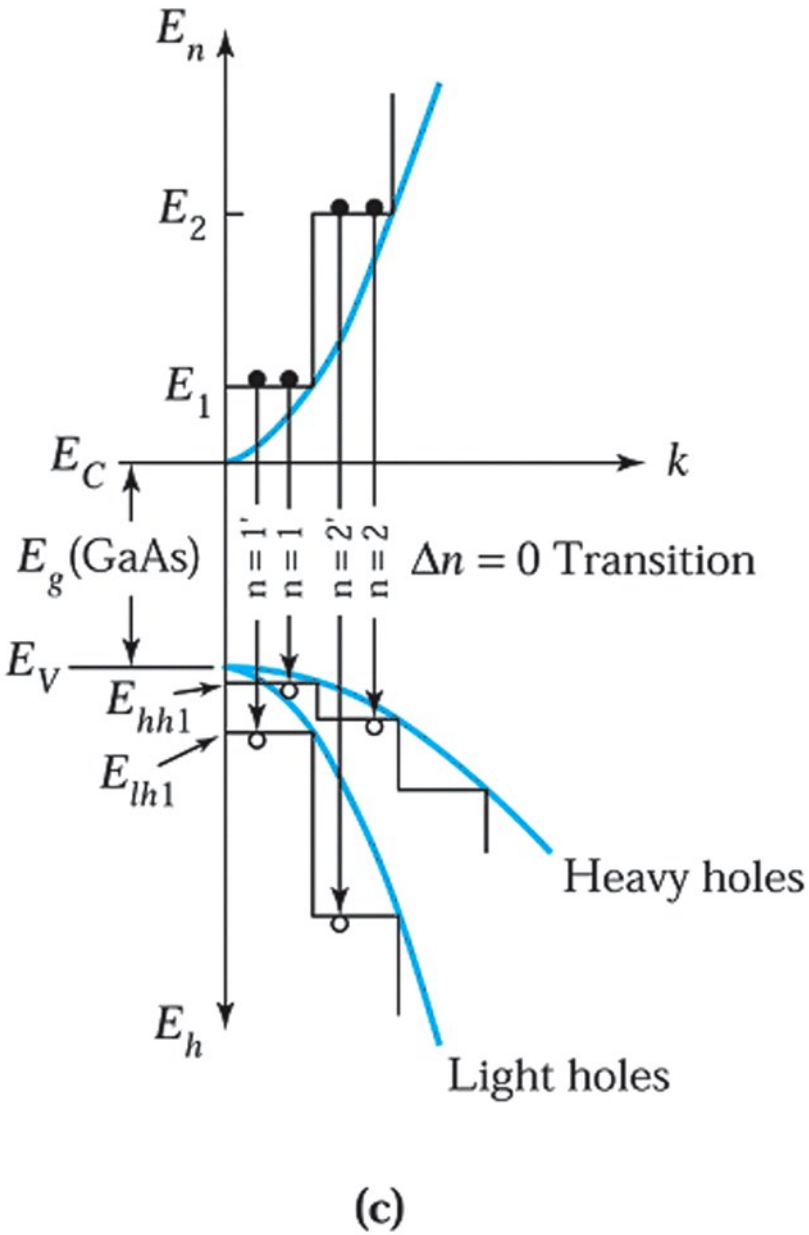

Figure 9.31c

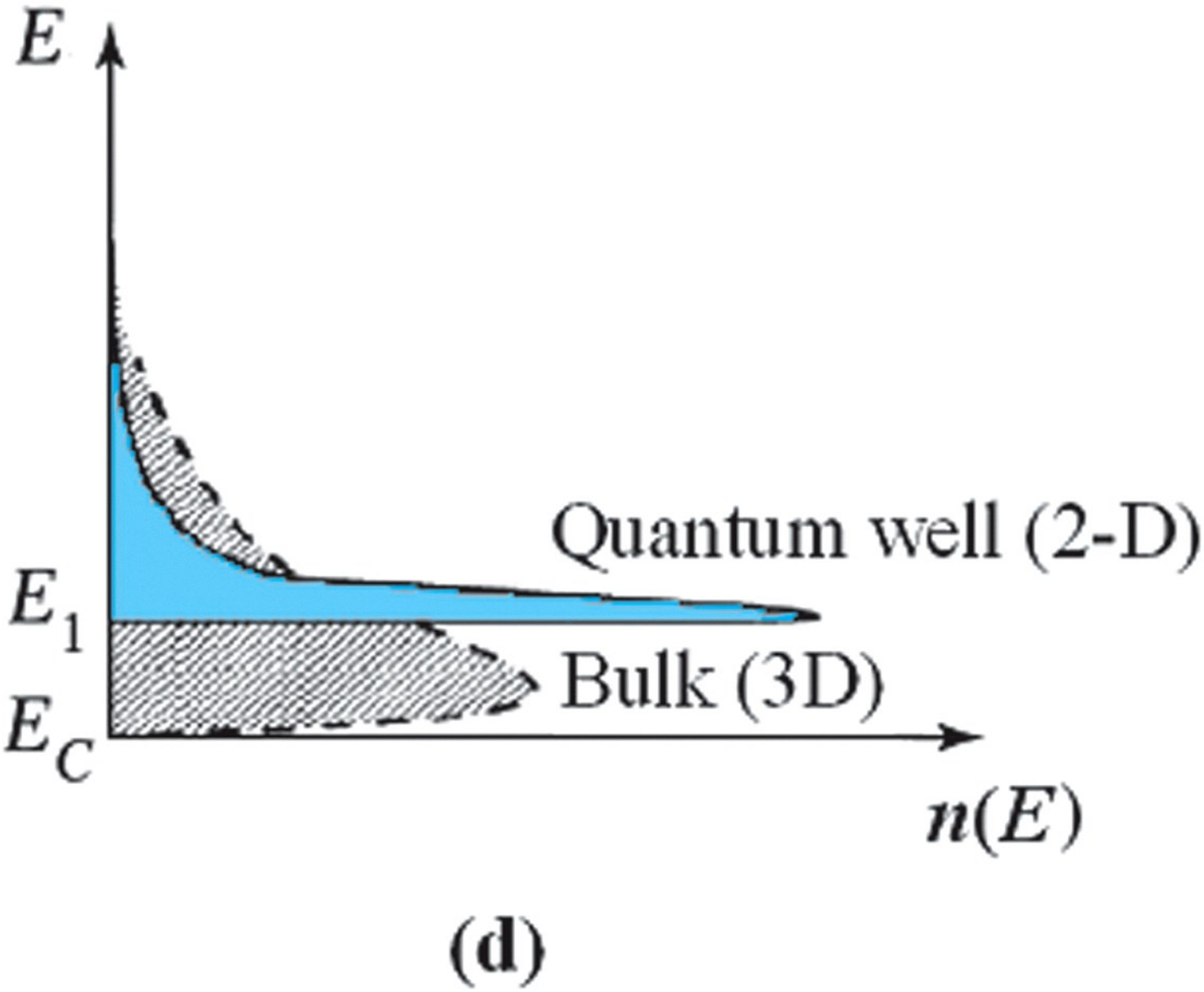

Figure 9.31d

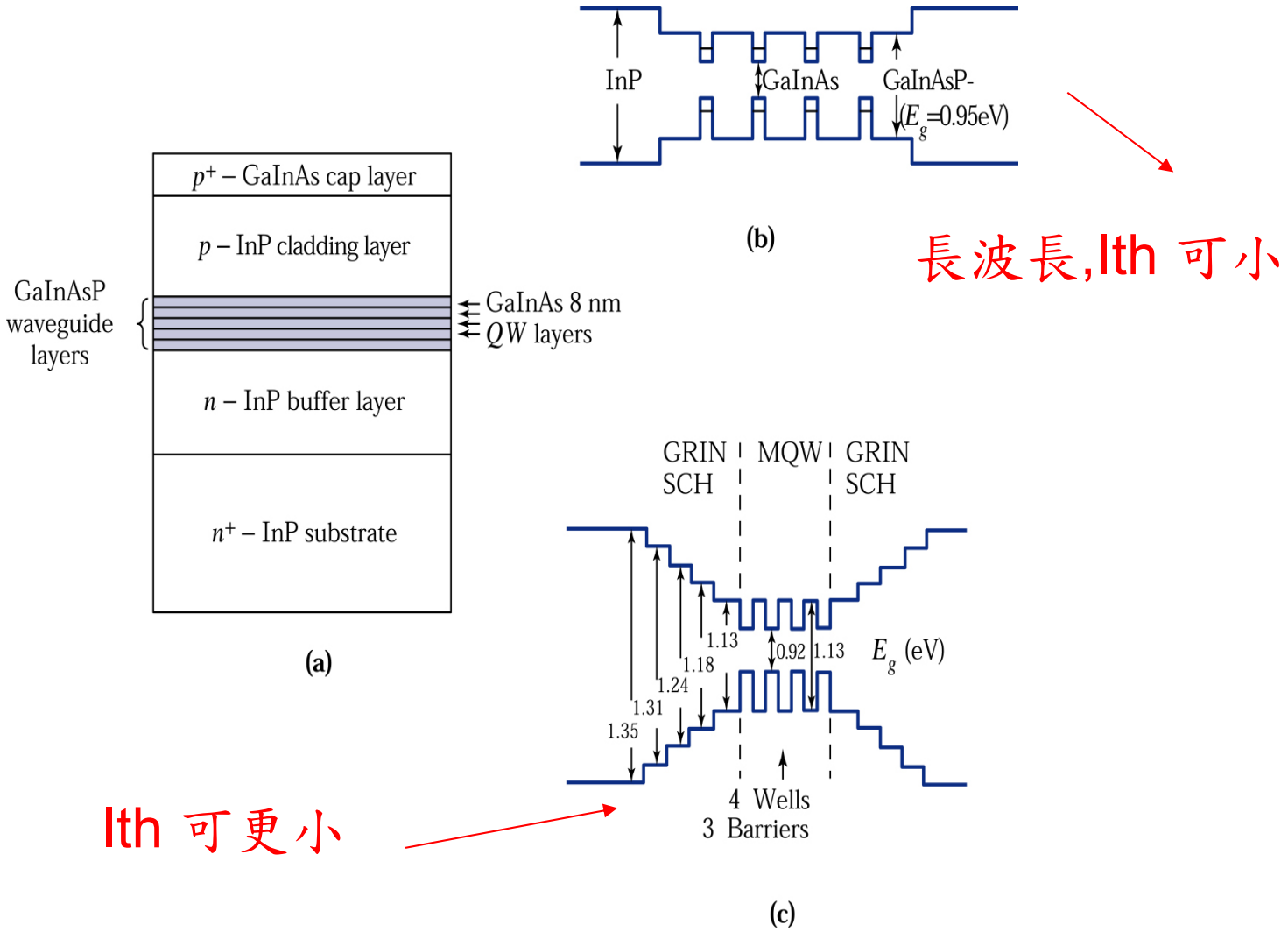

Figure 9.32. (*a*) Schematic of the cross-section of an GaInAs/GaInAsP multiple-quantum-well laser structure. (*b*) Schematic of the bandgaps of the SCH-MQW layers shown in (*a*). (*c*) GRIN-SCH-MQW structure with thin layers of increasing bandgaps to approximate the graded-index change.[20]

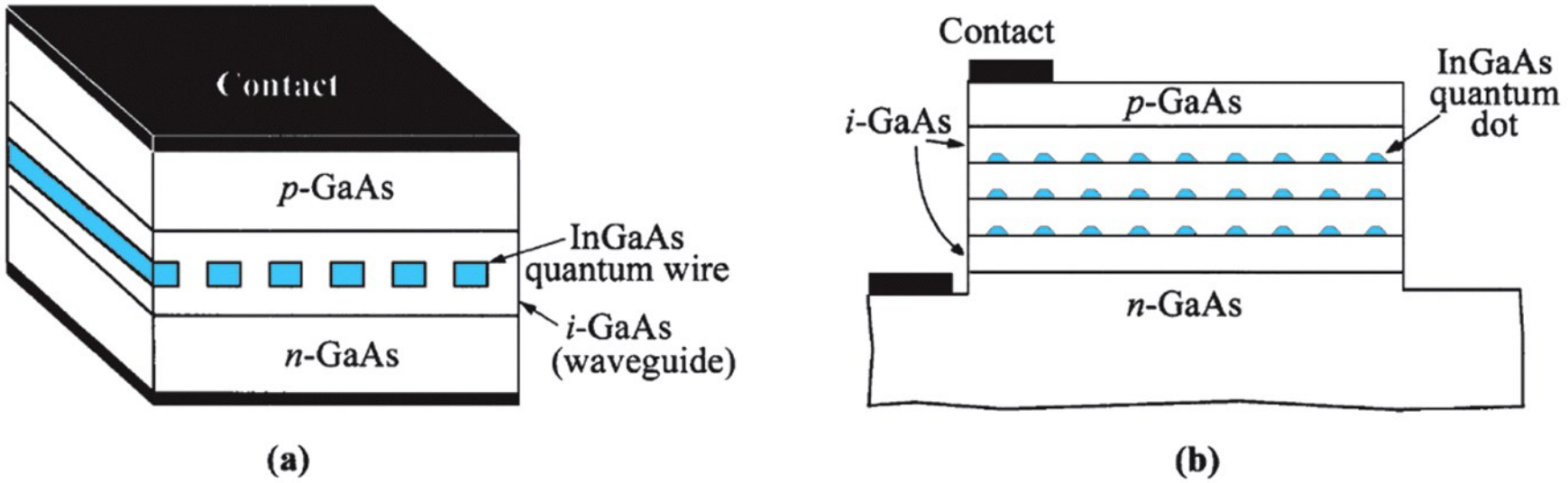

Figure 9.33

(a) Quantum-wire laser
(b) Quantum-dot laser

When dimension reduces, peak gain increases and has narrower spectrum

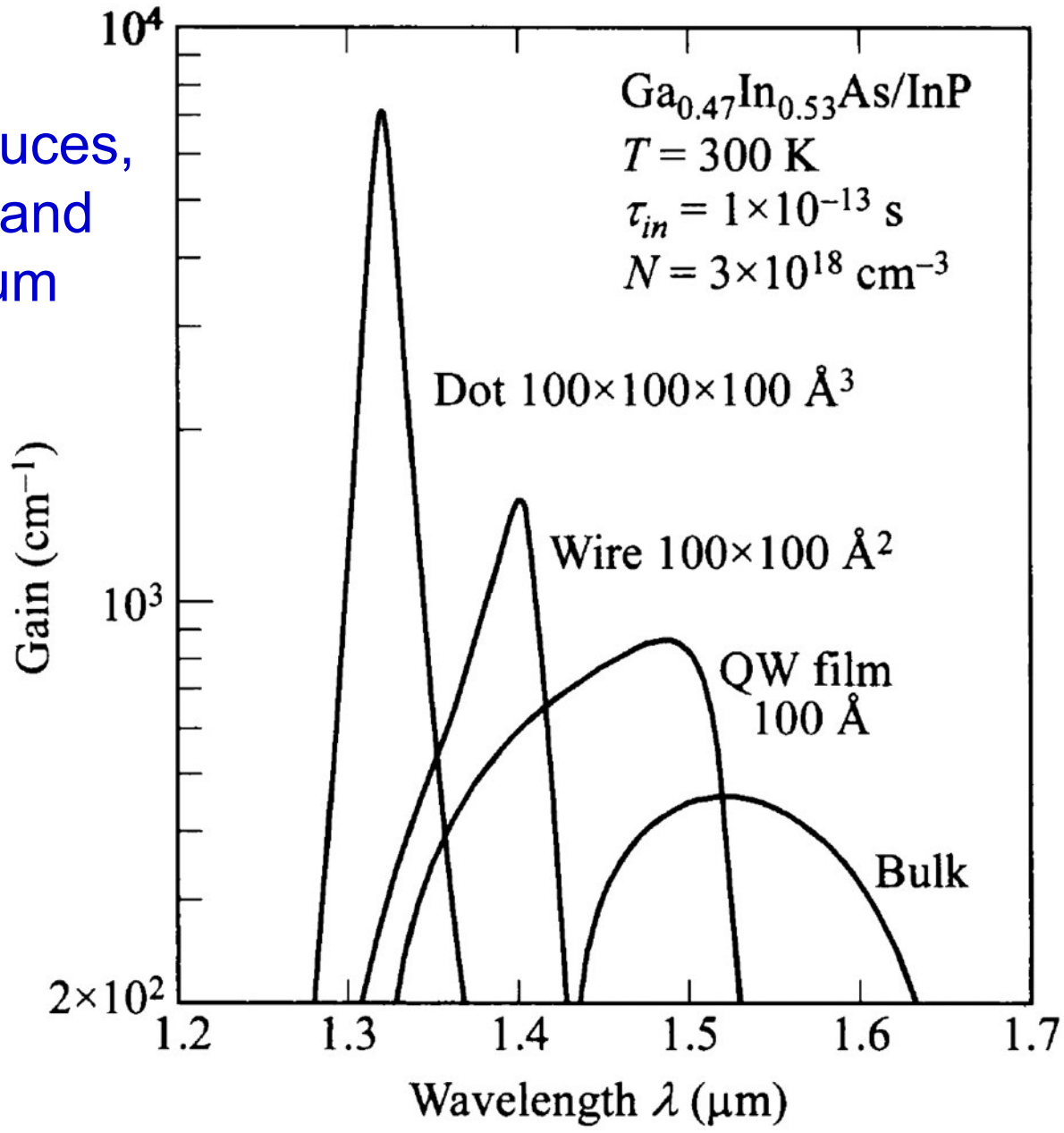

Figure 9.34

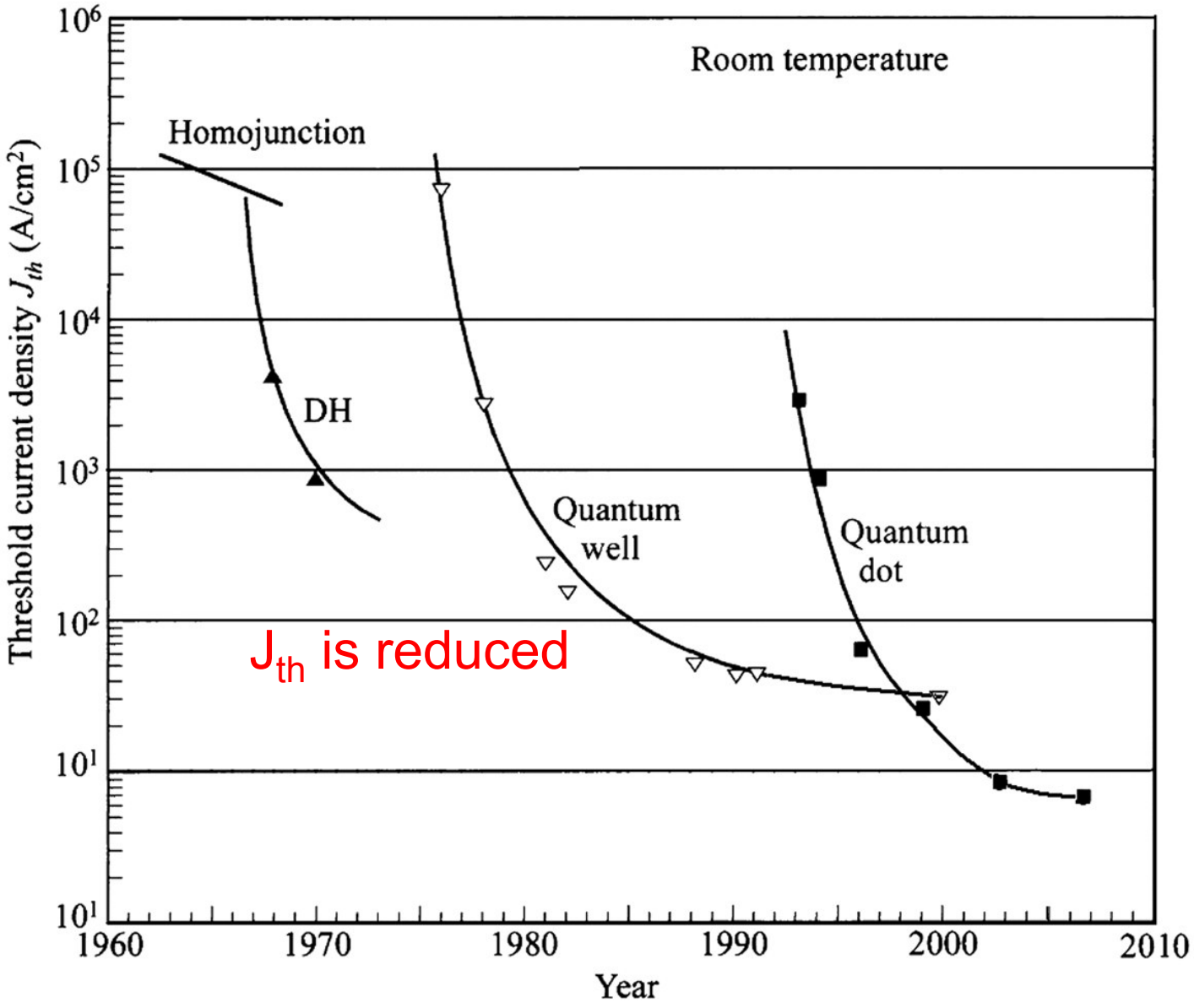

Figure 9.35

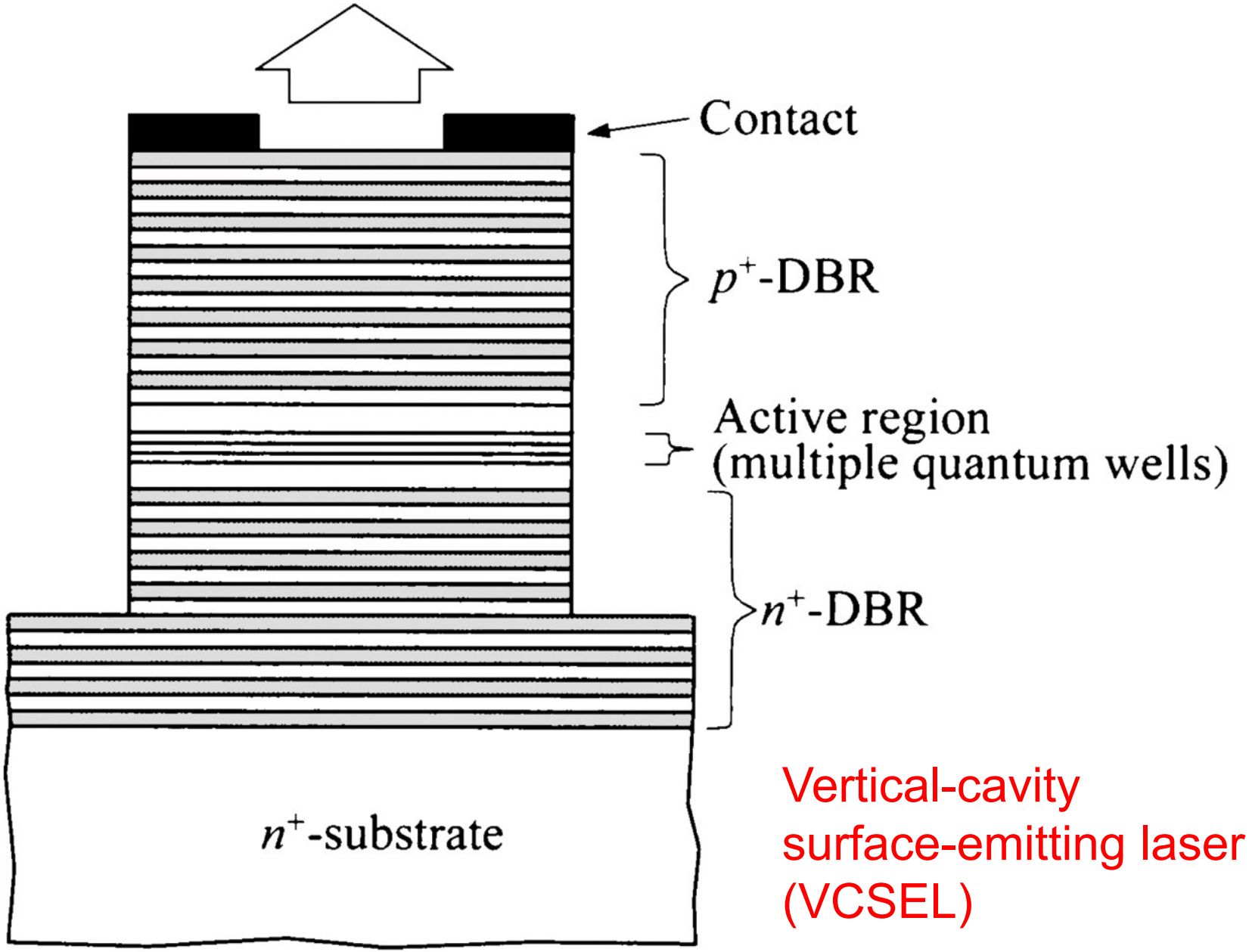

Vertical-cavity surface-emitting laser (VCSEL)

Figure 9.36

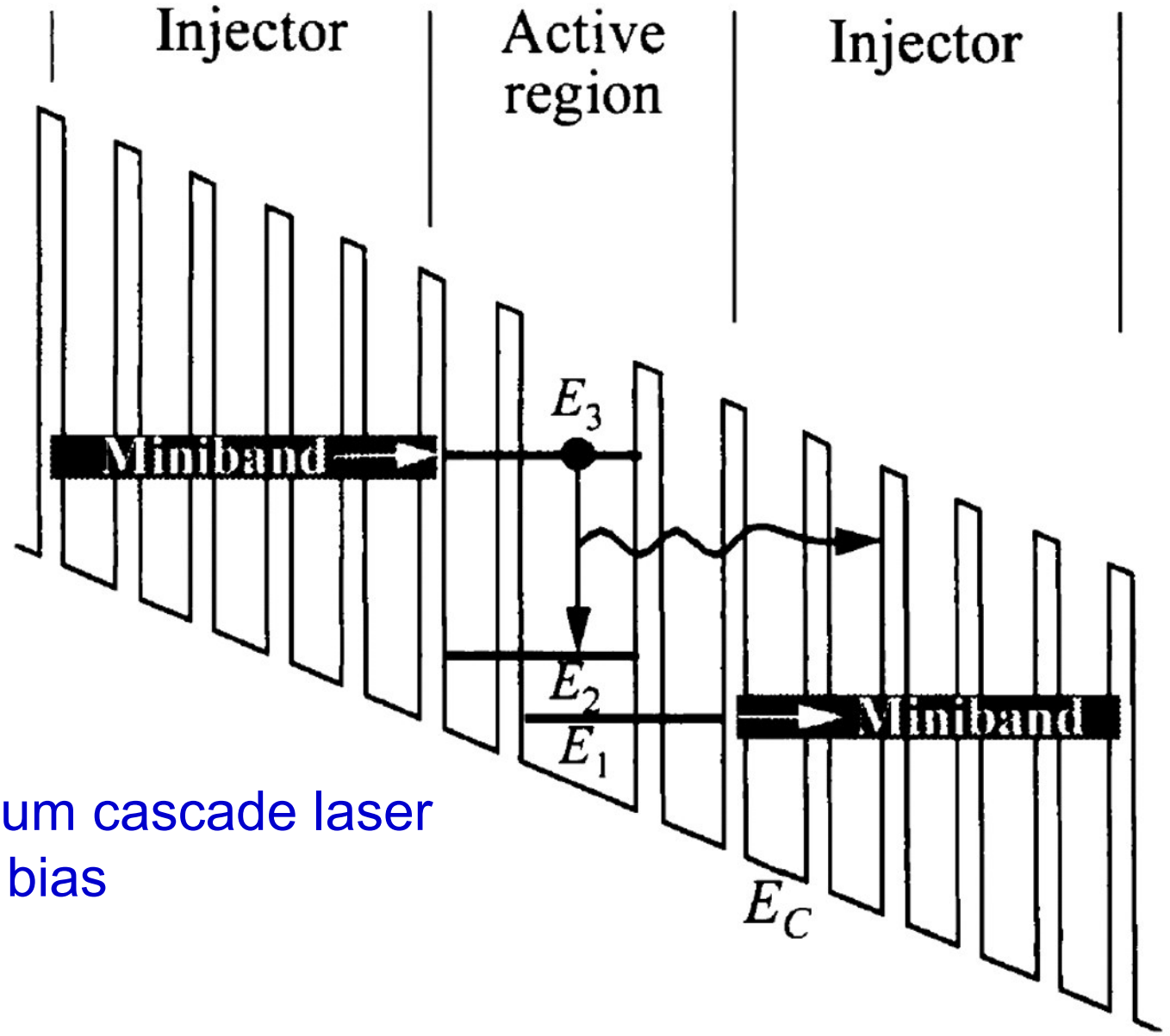

Quantum cascade laser under bias

Figure 9.37

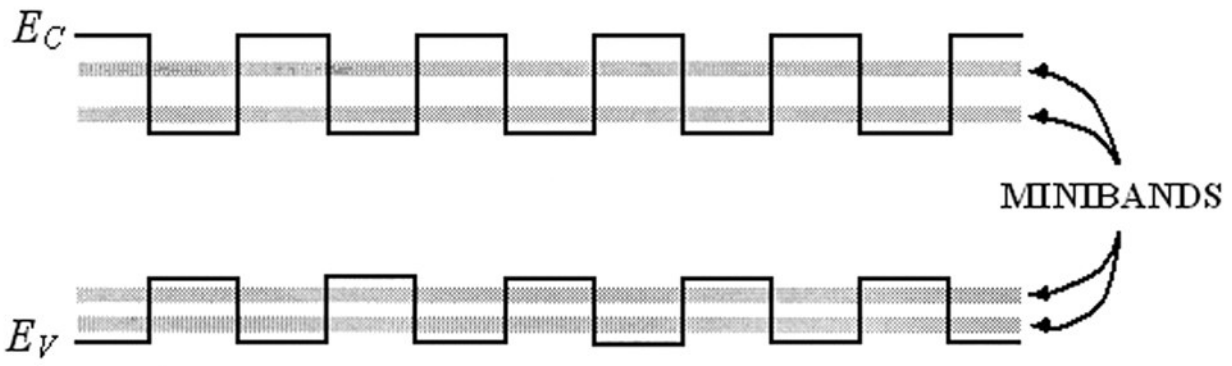

Figure 9.38

Hetero-structure superlattice